

ARTICLE TYPE

Structured Learning in Time-dependent Cox Models

Guanbo Wang^{†*1} | Yi Lian^{†2} | Archer Y. Yang^{*3,4} | Robert W. Platt⁵ | Rui Wang^{6,7} | Sylvie Perreault⁸ | Marc Dorais⁹ | Mireille E. Schnitzer^{8,10}

¹Department of Epidemiology, Harvard T.H. Chan School of Public Health, MA, U.S.A.

²Department of Biostatistics, Epidemiology and Informatics, University of Pennsylvania, PA, U.S.A.

³Department of Mathematics and Statistics, McGill University, QC, Canada

⁴Mila, Québec AI Institute, QC, Canada

⁵Department of Epidemiology, Biostatistics and Occupational Health, McGill University, QC, Canada

⁶Department of Population Medicine, Harvard Pilgrim Health Care Institute and Harvard Medical School, MA, U.S.A.

⁷Department of Biostatistics, Harvard T. H. Chan School of Public Health, MA, U.S.A.

⁸Faculté de pharmacie, Université de Montréal, QC, Canada

⁹StatSciences Inc. QC, Canada

¹⁰Département de médecine sociale et préventive, Université de Montréal, QC, Canada

[†] co-first author

Correspondence

*Guanbo Wang, Email: gwang@hsph.harvard.edu * Archer Y. Yang, Email: archer.yang@mcgill.ca

Present Address

677 Huntington Ave, Boston, MA 02115

Summary

Cox models with time-dependent coefficients and covariates are widely used in survival analysis. In high-dimensional settings, sparse regularization techniques are employed for variable selection, but existing methods for time-dependent Cox models lack flexibility in enforcing specific sparsity patterns (i.e., covariate structures). We propose a flexible framework for variable selection in time-dependent Cox models, accommodating complex selection rules. Our method can adapt to arbitrary grouping structures, including interaction selection, temporal, spatial, tree, and directed acyclic graph structures. It achieves accurate estimation with low false alarm rates. We develop the `sox` package, implementing a network flow algorithm for efficiently solving models with complex covariate structures. `sox` offers a user-friendly interface for specifying grouping structures and delivers fast computation. Through examples, including a case study on identifying predictors of time to all-cause death in atrial fibrillation patients, we demonstrate the practical application of our method with specific selection rules.

KEYWORDS:

Grouping structures, high-dimensional data, network flow algorithm, time-dependent Cox models, structured sparse regularization, structured variable selection, survival analysis

1 Introduction

The Cox model¹ is a well-established statistical model widely used for survival data analysis. Incorporating time-dependent covariates and coefficients in the Cox model offers more flexibility in representing associations between covariates and the hazard of the event of interest. Examples of time-varying covariates include medication usage² and disease status³. Integrating time-varying coefficients into the Cox model is particularly relevant in cases where the relationship between covariates and the outcome of interest changes over time.

In many real-world applications of time-dependent Cox models, the number of covariates can be very large, potentially exceeding the number of observations in the data. To address the challenges of model overfitting and perform variable selection in such high-dimensional settings, sparse regularization techniques can be employed. These techniques help remove redundant

covariates from the model and improve estimation/prediction accuracy. For example, LASSO and SCAD regularization methods have been extensively studied for Cox models^{4,5}. In the context of time-dependent covariates and coefficients, some variable selection methods in the Cox model have been proposed^{6,7}. However, these methods only select variables individually and do not enforce specific sparsity patterns on the covariates.

Investigators often have prior knowledge about the structure of potential model covariates, which imposes certain restrictions on how covariates should be included in the model. For example, strong heredity states that “if the interaction term is selected, then the main terms should also be selected”⁸. To incorporate such information, which we refer to as “selection rules”, a penalty can be applied to a weighted sum of the norms of group variable coefficients. Different specifications of grouping structures corresponds to different selection rules. In the context of Cox models without time-varying covariates or coefficients, various methods have been proposed to incorporate specific types of selection rules. For example, Wang et al.⁹ introduced methods to incorporate strong heredity in interaction selection, while Simon et al.¹⁰ and Wang et al.¹¹ developed sparse group LASSO techniques. Additionally, Dang et al.¹² extended the latent overlapping group LASSO¹³ to the Cox model, which requires specifying latent variables. Though the method can follow more types of selection rules, it is not scalable to high-dimensional settings with complex grouping structures due to the built-in algorithms. For instance, the method is not well studied when multi-layer groups (such as tree and graph structures) have significant overlap and the sparsity level is low¹⁴. To the best of our knowledge, no method or software is available for structurally selecting variables in time-dependent Cox models.

We contribute to this field of research in several ways. First, we propose the first application of the structured sparsity-inducing penalty¹⁵ to time-dependent Cox models. Our method can easily adapt to arbitrary grouping structures, allowing for the incorporation of highly complex selection rules. This flexibility enables the inclusion of various structures such as interaction selection, temporal, spatial, tree, and directed acyclic graph structures. Our estimator demonstrates low false alarm rates and high estimation accuracy.

Secondly, to reduce the computational burden caused by selecting time-dependent covariates with complex grouping structures required by our method, we develop a network flow algorithm that efficiently and effectively solves models with complex covariate structures. To ensure optimal efficiency, we implement this algorithm as an R package called `sox`, (stands for structured learning for time-dependent Cox)¹⁶, which is available on CRAN. Our software leverages established SPAMS packages and provides users with a user-friendly interface to specify arbitrary grouping structures. It has a C++ core and offers fast computational speed and reliable performance.

Finally, we provide examples that illustrate how to specify grouping structures to respect complex selection rules in practical scenarios. In particular, in a case study, we apply our developed method to identify significant predictors associated with the time to death by any cause among hospitalized patients with atrial fibrillation. In this analysis, we incorporate eight selection rules and demonstrate the rationale behind specifying the corresponding grouping structure.

The rest of the paper is organized as follows. In section 2, we introduce the proposed method. Section 3 illustrates the algorithm for `sox`, followed by implementation details in section 4. We then present the results of simulation studies to compare our method to unstructured variable selection in both low and high dimensional settings in section 5, and present the application of `sox` in the case study in section 6. We conclude with a discussion in section 7.

2 Model specification and structured penalization

Consider individual failure times T_i and censoring times C_i indexed by $i = 1, \dots, n$. We can observe only the time to either failure or censoring, whichever comes first, i.e. $U_i = \min(T_i, C_i)$ with censoring indicator $\delta_i = I(T_i \leq C_i)$. We also consider a possibly time-varying, p -vector-valued covariate process $\mathbf{X}_i(t) = (X_{i1}(t), \dots, X_{ip}(t))^T$. We assume noninformative censoring, i.e. upon conditioning on $\mathbf{X}_i(t)$, C_i is independent of T_i . Therefore the observed data associated with n individuals are n triplets $\{U_i, \delta_i, \mathbf{X}_i(t)\}$ for $i = 1, \dots, n$, which we assume to be independently drawn from a common distribution. Denote by $h(t|\cdot)$ the covariate-conditional hazard function; we assume that $h_i(t) = h_0(t) \cdot \exp\{\mathbf{X}_i(t)^T \boldsymbol{\beta}\}$, where $h_0(\cdot)$ is an unspecified baseline hazard function. We begin by considering the scenario in which the coefficient vector, denoted as $\boldsymbol{\beta} \in \mathbb{R}^p$, is time-invariant. Subsequently, we will explore the case of time-varying coefficients.

To handle tied-events, we define an index $\ell = 1, \dots, L$ for the ordered unique follow-up times in the dataset, and an ordered list $t_1 < t_2 < \dots < t_L$ of unique time-to-event realizations. The number of tied events occurring at the ℓ th distinct survival time is denoted by d_ℓ . We can further define two index sets, D_ℓ and R_ℓ , representing the subjects whose event occurred at time t_ℓ and were at risk at time t_j , respectively. Using the Breslow approximation to accommodate tied events¹⁷, the negative log partial

likelihood can be approximated as

$$f(\boldsymbol{\beta}) \approx - \sum_{\ell=1}^L \left(\left\{ \sum_{i \in D_\ell} \mathbf{X}_i(t_\ell)^\top \right\} \boldsymbol{\beta} - d_\ell \log \left[\sum_{i \in R_\ell} \exp\{\mathbf{X}_i(t_\ell)^\top \boldsymbol{\beta}\} \right] \right). \quad (\text{S1})$$

Up until now, we assume the coefficients $\boldsymbol{\beta}$ are time-invariant, but there are several ways to accommodate the case where $\boldsymbol{\beta}$ depends on time t . For example, for $j = 1, \dots, p$, let $\beta_j(t)$ be $\sum_{m=1}^M I(T_m \leq t < T_{m+1}) \beta_{jm}$ (with specified time intervals $[T_m, T_{m+1})$, $m = 1, \dots, M$) or $a_j + b_j \log(t)$, as functions of t . More flexibly, let $\beta_j(t) = \sum_{m=1}^M \theta_{jm} \phi_m(t)$, where $\phi_m(\cdot)$ is a set of B-spline basis functions for approximating the function $\beta_j(t)$. The problem of estimating $\beta_j(t)$ is then transformed to the problem of estimating $a_j, b_j, \boldsymbol{\beta}_j = (\beta_{j1}, \dots, \beta_{jm})^\top$, or $\boldsymbol{\theta}_j = (\theta_{j1}, \dots, \theta_{jM})^\top$. For the sake of simplicity, we adopt the notation of time-invariant coefficients, as given in equation (S1), as the primary framework in this paper. But we note that Cox models with time-dependent coefficients can be viewed as a specific instance in the broader context. For a detailed explanation, please refer to Example A.3.

To incorporate a selection rule into selecting time-dependent covariates, one approach is to enforce the collective selection of groups of covariates. However, some previous approaches have imposed restrictions on the grouping structure^{18,10}, such as the prohibition of overlap between groups. In contrast, this work adopts a flexible approach by imposing no constraints on the grouping structure, allowing for the consideration of a wider range of selection rules¹⁵. Let $\mathbb{V}(t) = \{X_1(t), X_2(t), \dots, X_p(t)\}$ denote the set containing all the covariates (for the brevity, we will use \mathbb{V} throughout the paper). Suppose there are K pre-defined groups of these covariates, and let us define the grouping structure as $\mathbb{G} = \mathfrak{g}_k, k = 1 \dots, K$, where \mathfrak{g}_k represents a group – a non-empty subset of \mathbb{V} – and the union of all \mathfrak{g}_k 's is equal to \mathbb{V} . It is worth noting that the groups can overlap, meaning that $\mathfrak{g}_j \cap \mathfrak{g}_k$ may not be empty for $j \neq k$. To denote a vector of the same length as $\boldsymbol{\beta}$, with non-zero entries corresponding to the covariates in \mathfrak{g} and zero entries elsewhere, we use $\boldsymbol{\beta}_{|\mathfrak{g}}$.

To select variables according to the pre-defined groups to achieve structural selection in time-dependent Cox models, we solve the following problem

$$\min_{\boldsymbol{\beta}} f(\boldsymbol{\beta}) + \lambda \Omega(\boldsymbol{\beta}), \quad \Omega(\boldsymbol{\beta}) = \sum_{\mathfrak{g} \in \mathbb{G}} \omega_{\mathfrak{g}} \left\| \boldsymbol{\beta}_{|\mathfrak{g}} \right\|_q. \quad (\text{S2})$$

Here, $f(\boldsymbol{\beta})$ is a convex differentiable function as defined in Equation (S1). The weight $\omega_{\mathfrak{g}}$ is a positive user-defined value associated with the group \mathfrak{g} , and $\Omega(\boldsymbol{\beta})$ represents the weighted sum of sparsity-inducing ℓ_q norms ($q = 2$ or ∞) applied to groups of coefficients $\boldsymbol{\beta}_{|\mathfrak{g}}$, where $\mathfrak{g} \in \mathbb{G}$. The choice of norm can be either the ℓ_∞ norm (which corresponds to the maximum absolute value of $\boldsymbol{\beta}_{|\mathfrak{g}}$) or the ℓ_2 norm. Both norms serve the purpose of encouraging the collective selection of a group of variables. However, in this paper, we primarily focus on the piece-wise linear ℓ_∞ norm.

By employing this type of penalization, each group of variables can be excluded from the model as a group, thereby promoting sparsity. The specifications of the grouping structure \mathbb{G} , determining the membership of variables in each group \mathfrak{g} , leads to different sets of variables that can be selected (i.e., the complement of the union of the groups). This allows for incorporating various a priori knowledge or structures exhibited in the real data. Importantly, we allow for the inclusion of highly overlapped groups, enabling the inclusion of a wide range of structures.

To operationalize the structures in a mathematical and explicit manner, we initially translate them into selection rules, which represent the dependencies among variables. Subsequently, we specify the grouping structure \mathbb{G} to adhere to these selection rules. This approach allows us to articulate and identify the structures to be incorporated effectively. While we do not delve into the detailed explanation in this article, interested readers can find further information in existing literature^{19,20}.

Various types of selection rules can be followed by the structured sparsity-inducing penalty, such as strong heredity, temporal and spatial structures, and rules that require tree or graph grouping structures. In A, we provide five detailed examples of such selection rules and their related grouping structure specifications. More examples of selection rules can be found in¹⁵ and²¹.

In the next section, we present an efficient algorithm for solving the objective function (S2) for time-dependent Cox models, allowing for the incorporation of selection rules that can be followed by the structured sparsity-inducing penalty.

3 Proximal gradient with network flow algorithm

In this section, we illustrate the use of a proximal gradient algorithm²² with network flow to solve (S2) with a structural penalty.

Since $\Omega(\boldsymbol{\beta})$ is not differentiable on its entire support, the optimization of the penalized likelihood requires the proximal method. The proximal method²³ has been successfully applied in various research areas, including signal processing²⁴ and machine learning²⁵.

To address the computational challenge posed by the non-smooth component in the objective function, the proximal method updates estimates that remain close to the gradient update for the differentiable function $f(\boldsymbol{\beta})$, while also minimizing the non-differentiable penalty term²⁶. This approach enjoys a linear convergence rate^{27,28}. More specifically, the updated value of $\boldsymbol{\beta}$ in each iteration of the proximal gradient algorithm, denoted as $\boldsymbol{\beta}^+$, is obtained by minimizing the following approximated problem. Here, the loss function f is approximated by a quadratic function:

$$\begin{aligned}\boldsymbol{\beta}^+ &= \underset{\boldsymbol{\beta}}{\operatorname{argmin}} f(\tilde{\boldsymbol{\beta}}) + (\boldsymbol{\beta} - \tilde{\boldsymbol{\beta}}) \nabla f(\tilde{\boldsymbol{\beta}}) + \frac{1}{2q} \|\boldsymbol{\beta} - \tilde{\boldsymbol{\beta}}\|_2^2 + \lambda \Omega(\boldsymbol{\beta}) \\ &= \underset{\boldsymbol{\beta}}{\operatorname{argmin}} \frac{1}{2q} \|\boldsymbol{\beta} - \{\tilde{\boldsymbol{\beta}} - q \nabla f(\tilde{\boldsymbol{\beta}})\}\|_2^2 + \lambda \Omega(\boldsymbol{\beta}),\end{aligned}$$

where $\tilde{\boldsymbol{\beta}}$ is the value of $\boldsymbol{\beta}$ from the previous iteration, and t is the step size of the update. By defining $\mathbf{u} = \tilde{\boldsymbol{\beta}} - q \nabla f(\tilde{\boldsymbol{\beta}})$, the above problem can be further written as

$$\boldsymbol{\beta}^+ = \operatorname{prox}_{q\lambda\Omega} \{\tilde{\boldsymbol{\beta}} - q \nabla f(\tilde{\boldsymbol{\beta}})\} := \underset{\boldsymbol{\beta}}{\operatorname{argmin}} \frac{1}{2} \|\boldsymbol{\beta} - \mathbf{u}\|_2^2 + q\lambda \sum_{\mathfrak{g} \in \mathbb{G}} \omega_{\mathfrak{g}} \|\boldsymbol{\beta}_{|\mathfrak{g}}\|_{\infty}. \quad (\text{S3})$$

In many cases, the proximal operator can be computed in a closed form, leading to efficient computations. However, for more complex structures such as nested groups (e.g., tree structures) or general directed acyclic graphs (e.g., Example A.1 and the first one in Example A.3), the closed-form proximal operator may not exist. In the case of a tree structure, the proximal operator can still be efficiently computed using its dual form in a blockwise coordinate ascent fashion²⁹. However, dealing with general directed acyclic graphs presents a greater challenge. To address this issue, Marial et al.²¹ converted the dual form of the proximal operator into a quadratic min-cost flow problem, enabling efficient computations in the context of such graphs.

Define the dual variables $\boldsymbol{\xi}_{|\mathfrak{g}}$, which satisfies $\sum_{\mathfrak{g} \in \mathbb{G}} \boldsymbol{\xi}_{|\mathfrak{g}} = \boldsymbol{\beta}$.

The dual of problem (S3),

$$\min_{\boldsymbol{\xi}} \frac{1}{2} \left\| \mathbf{u} - \sum_{\mathfrak{g} \in \mathbb{G}} \boldsymbol{\xi}_{|\mathfrak{g}} \right\|_2^2, \quad \text{s.t. } \forall \mathfrak{g} \in \mathbb{G}, \|\boldsymbol{\xi}_{|\mathfrak{g}}\|_1 \leq \lambda \omega_{\mathfrak{g}} \text{ and } \xi_{|\mathfrak{g},j} = 0 \text{ if } j \notin \mathfrak{g}, \quad (\text{S4})$$

can be transformed into a quadratic min-cost flow problem³⁰. This conversion allows us to efficiently solve the problem using a network flow algorithm based on the mini-cut theorem³¹. The algorithm converges in a finite and polynomial number of operations, providing an effective solution to the dual problem.

The network flow algorithm, commonly used in graph models³², has found widespread application in various machine learning domains, such as in image processing³³. Because of the special form of the constrain in our problem, we are able to present a more efficient version of the algorithm²¹, referred to as Algorithm 1, for solving (S4). The central computation in the algorithm is the evaluation of $\sum_{\mathfrak{g} \in \mathbb{G}} \boldsymbol{\xi}_{|\mathfrak{g}}$, accomplished by the `computeFlow` function. The details of the algorithm's steps are presented in B.

The algorithm is equivalent to the network flow algorithm²¹, but with a different presentation style. Our presentation connects to the general framework for structured variable selection and is consistent with the research problem in our context.

4 Implementation details

We provide an efficient and user-friendly R package `sox`, which is available on CRAN (<https://cran.r-project.org/package=sox>). The statistical software is implemented in C++ with the incorporation of programs adapted from well-established software packages including the `survival`³⁴, `glmnet`^{35,36} and `SPAMS`²¹ to ensure optimal efficiency. It provides users with a convenient interface to specify the grouping structure relevant to their specific data analysis task. In addition, the `sox` features built-in solution path and cross-validation functions with their corresponding visualization tools to facilitate model tuning and diagnostics.

Details of implementing the max flow algorithm.

Algorithm 1 Solving (S4) using quadratic min-cost flow

Inputs: The estimate in the k th step $\beta^k \in \mathbb{R}^p$, step size q , \mathbb{V} , \mathbb{G} , ω_g , λ . Set $\xi = 0$.

Compute $\sum_{g \in \mathbb{G}} \xi_{|g} \leftarrow \text{computeFlow}(\mathbb{V}, \mathbb{G})$.

return $\beta^k - q \nabla f(\beta^k) - \sum_{g \in \mathbb{G}} \xi_{|g}$

Function $\text{computeFlow}(\mathbb{V}, \mathbb{G})$

Projection: $\gamma \leftarrow \text{argmin}_{\gamma} \sum_{j: X_j \in \mathbb{V}} \frac{1}{2t} (\beta_j^k - q \nabla f(\beta_j^k) - \gamma_j)^2$ s.t. $\sum_{j: X_j \in \mathbb{V}} \gamma_j \leq \lambda \sum_{g \in \mathbb{G}} \omega_g$

Updating: $(\sum_{g \in \mathbb{G}} \xi_{|g}^j)_{X_j \in \mathbb{V}} \leftarrow \text{argmax}_{(\sum_{g \in \mathbb{G}} \xi_{|g}^j)_{X_j \in \mathbb{V}}} \sum_{X_j \in \mathbb{V}} \sum_{g \in \mathbb{G}} \xi_{|g}^j$ s.t. $\sum_{X_j \in \mathbb{V}} \xi_{|g}^j \leq \lambda \omega_g$

Recursion:

if $\exists X_j \in \mathbb{V}$ s.t. $\sum_{g \in \mathbb{G}} \xi_{|g}^j \neq \gamma_j$ **then**

Denote $\mathbb{V}^* = \{X_j \in \mathbb{V} : \sum_{g \in \mathbb{G}} \xi_{|g}^j = \gamma_j\}$, and $\mathbb{g}^* = \{g \in \mathbb{G} : \sum_{X_j \in \mathbb{g}} \xi_{|g}^j < \lambda \omega_g\}$

$(\sum_{g \in \mathbb{G}} \xi_{|g}^j)_{X_j \in \mathbb{V}^*} \leftarrow \text{computeFlow}(\mathbb{V}^*, \mathbb{G}^*)$

$(\sum_{g \in \mathbb{G}} \xi_{|g}^j)_{X_j \in \mathbb{V} \setminus \mathbb{V}^*} \leftarrow \text{computeFlow}(\mathbb{V} \setminus \mathbb{V}^*, \mathbb{G} \setminus \mathbb{G}^*)$

end

return $(\sum_{X_j \in \mathbb{g}} \xi_{|g}^j)_{X_j \in \mathbb{V}}$

We utilize the max flow algorithm, as proposed by Goldberg and Tarjan³⁷, for the efficient execution of the updating step within the `computeFlow` process. To our knowledge, it remains unmatched in terms of speed and effectiveness for solving max-flow problems. The algorithm has a worst-case complexity of $O(|V|^2|E|^{1/2})$ ³⁸, and is well-suited for efficient distributed and parallel implementations. This algorithm has been effectively integrated into our package `sox`, using the SPAMS packages with a C++ core. In the following section, we provide a concise introduction to this algorithm.

Consider a canonical graph where each node $v \in V$ can be a source s_1 , and sink s_2 , a single variable ($X_j \in \mathbb{V}$), or a set of variables ($\mathbb{g}_k \in \mathbb{G}$), that is, $V = \{s_1, s_2\} \cup \mathbb{V} \cup \mathbb{G}$. In addition, there is an arc $e \in E \subseteq V \times V$ from s_1, \mathbb{g}_k , and X_j to \mathbb{g}_k, X_j , and s_2 respectively. From one vertex v to another w , each arc has attributes such as non-negative functions of flow $f(v, w)$, which equals $-f(w, v)$, capacity $c(v, w) \geq f(v, w)$, the flow excess $h(v) = \sum_{u \in V} f(u, v) \geq 0, \forall v \in \{V - \{s_1\}\}$, and the residual capacity $r(v, w) = c(v, w) - f(v, w)$. See Table S1 for the definitions of those functions. Therefore, the updating step in Algorithm 1 can be formulated as “finding the maximum value of the flow while ensuring that the flow on each arc does not exceed its capacity”.

There are two basic operations in the max flow algorithm. One is *push*, which pushes the excess from v to w by $\min\{h(v), r(v, w)\}$ when $h(v) > 0$ and $r(v, w) > 0$. The other is *relabel*, which estimates the distance from a vertex v to the sink s_2 . Define the distance as $d(v)$, where $d(s_1) = |V|$. Relabeling updates the $d(v)$ to $\min\{d(w) + 1 | r(v, w) > 0, d(v) < d(w)\}$.

The algorithm first initializes and relabels the distance, and then pushes excess from the vertex whose flow equals the capacity on each edge and can reach the sink to vertices that have a shorter estimated distance to the sink s_2 , with the goal of getting as much excess as possible to s_2 . When a vertex cannot reach the sink with a positive excess, the algorithm pushes such excess in the opposite direction. In each update, the value of the flow function is changed. Eventually, all vertices other than the source and sink have zero excess while each arc respects the capacity. At this point, the flow is a maximum flow, and thus, the value of the flow function can be computed as the updated value in the updating step in Algorithm 1.

Backtracking line search.

The proposed algorithm for solving the dual of the proximal operator includes the step size q , which enables the incorporation of backtracking line search. The algorithm, presented in Algorithm 2, allows us to solve (S3) using proximal gradient descent with backtracking line search³⁹. Backtracking line search is an optimization technique that helps determine the appropriate step size. It begins with a predefined step size for updating along the search direction and iteratively shrinks the step size (i.e., “backtracks”) until the decrease in the loss function corresponds reasonably to the expected decrease based on the local gradient of the loss function. This technique enhances the convergence speed of the algorithm.

In our implementation, the step size shrinkage rate α is a parameter in the backtracking line-search that controls the rate at which the step size is reduced during each iteration of line-search until an appropriate step size is found. The proper step size should satisfy the line-search criteria, ensuring that the update with this step size leads to a sufficient decrease in the objective function. If α is too large, the step size might not reduce sufficiently during each iteration of the line search, which can cause the line search algorithm to take more iterations to find an appropriate step size. On the other hand, if the shrinkage factor is too small, it may lead to an over-reduction of the step size, resulting in a small update and slow convergence of the algorithm. In

Algorithm 2 Solving (S3) using proximal gradient descent with backtracking line search

Inputs: $X_i(t)$, T_i , δ_i , \mathbb{V} , \mathbb{G} , $\omega_{\mathbb{G}}$, λ , convergence threshold r , shrinkage rate $\alpha < 1$, step size q . Set $\beta^0 = \mathbf{0}$, $k = 0$.

repeat

$$\beta^+ \leftarrow \text{prox}_{q\lambda\Omega}(\beta^k - q\nabla f(\beta^k))$$

▷ call Algorithm 1

$$\text{if } f(\beta^+) \leq f(\beta^k) + \nabla f(\beta^k)^\top(\beta^+ - \beta^k) + \frac{1}{2q} \|\beta^+ - \beta^k\|_2^2 \text{ then}$$

$$k = k + 1; \beta^{k+1} \leftarrow \beta^+$$

exit;

else

$$q \leftarrow \alpha q$$

end

until $\|\beta^k - \beta^{k-1}\|_1 < r$;

return $\hat{\beta} \leftarrow \beta^{k+1}$

our implementation, we have chosen the commonly used default value of $\alpha = 0.5$ as the shrinkage rate. This choice has proven to be effective for all computations in our simulations and real data analysis.

Cross-validation.

We employ cross-validation to select the appropriate value of λ . The average cross-validated error (CV-E) is utilized for this purpose. Consider performing L -fold cross-validation, where we denote $\hat{\beta}^{-l}$ as the estimate obtained from the remaining $L-1$ folds (training set). The error of the l -th fold (test set) is defined as $2(P - Q)/R$, where P is the log partial likelihood evaluated at $\hat{\beta}^{-l}$ using the entire dataset, Q is the log partial likelihood evaluated at $\hat{\beta}^{-l}$ using the training set, and R is the number of events in the test set.

We opt for using the error defined above instead of the negative log partial likelihood evaluated at $\hat{\beta}^{-l}$ using the test set because it efficiently leverages the risk set, resulting in greater stability when the number of events in each test set is small. The CV-E serves as a metric for parameter tuning. Additionally, to account for the outcome balance among randomly formed test sets, we divide the deviance $2(P - Q)$ by R .

A note on the ‘‘One Standard Error Rule’’

Different values of λ correspond to different models in the regularization framework. The selection of the appropriate λ value is achieved through cross-validation.

When the objective is to identify the model with the lowest prediction error, we choose the value of λ that yields the lowest CV-E. This approach is known as the *min* rule³⁵. However, if the goal is to recover the sparsity pattern, meaning to select the set of variables that closely resembles the true model’s variable set, an alternative rule called the ‘‘one-standard-error-rule’’ (*Ise* rule) is recommended⁴⁰. The *Ise* rule selects the most parsimonious model whose prediction error is within one standard error of the minimum CV-E. By applying the *Ise* rule, we prioritize models that are more sparse while still maintaining reasonable prediction accuracy.

If the time-dependent covariates are internal covariates⁴¹, using the time-dependent Cox model for prediction may not be appropriate. However, when the objective is predictor identification, we recommend applying the *Ise* rule.

5 Simulation

We conduct several simulation studies. We evaluate our method in both low- and high-dimensional settings and test its performance in terms of the ability to strictly respect complex selection rules, selection consistency, estimation and prediction accuracy. We also compare our methods with the LASSO, the sparse group LASSO, and the latent overlapping group LASSO. In addition, we report the computation time, evaluate the cross-validation stability, and give insights into the influence of effect of group size, the amount of overlap, and sparsity levels on the performance of our method. All simulations employ 10-fold cross-validation to evaluate the performance. The simulations were conducted using R version 4.0.5⁴². The R code for simulation is available at https://github.com/Guanbo-W/sox_sim.

5.1 Categorical interaction selection under the time-dependent, low-dimensional setting

In the simulation, we generate data with three main terms, two of which are categorical variables, and two interactions between categorical variables. The three independent variables, $A(t)$, $B(t)$, and $C(t)$, are generated with values that randomly change over time in a piece-wise constant fashion. We consider 50 time points at which the values of any variable can potentially change, with each variable being held constant for a random duration between 5 and 10 time points. To simplify the notation, we use shorthand representations such as A to denote $A(t)$ (similarly for B and C). The categorical variables A and C are three-level variables represented by two dummy variables, denoted as A_1, A_2, C_1 , and C_2 , respectively. The variable B is continuous.

Hence, we consider the covariates and functions of covariates as follows $\mathbf{X} = \{A_1, A_2, B, A_1B, A_2B, C_1, C_2, C_1B, C_2B\}$. The below steps outline the procedure for generating A and C . Step 1, with replacement, sample 10 integers from $\{1, 2, 3\}$ with equal probability to represent the three categories of the variables; Step 2, for each sampled value, repeats the value R_i times, where R_i is sampled from $\{5, 6, \dots, 10\}$ with equal probabilities. Then, concatenate these repeated values together, resulting in a single vector with a length between 50 and 100; Step 3, take the first 50 elements as the values of the categorical variable. B is generated similarly, with the only difference being that in Step 1, we generate a series of numbers from a standard normal distribution. The time-to-event outcome is generated using a permutation algorithm implemented in the R function `PermAlgo`⁴³. The event times are dependent on the time-dependent potential predictors \mathbf{X} according to the Cox model, where $\beta^{9 \times 1}$ represents the vector of log hazard ratios of the predictors. The generated data included approximately 50% random censoring, meaning that for about half of the observations, the event time is unknown due to censoring. Among those not censored, the median event time occurred at approximately time 25. Two scenarios were evaluated:

Scenario 1: Only A_1 and A_2 are predictive of the outcome; their coefficients are set as $\log(3)$. This represents a sparse structure.

Scenario 2: There are five true predictors (A_1, A_2, B, A_1B, A_2B) that were predictive of the outcome; all of their coefficients are set as $\log(3)$. This corresponds to a less sparse structure.

To enforce selection rules strong heredity (selection rule 1) and “the binary indicators representing a categorical variable are selected collectively” (selection rule 2), we defined a grouping structure as $\{\{A_1, A_2, A_1B, A_2B\}, \{B, A_1B, A_2B, C_1B, C_2B\}, \{A_1B, A_2B\}, \{C_1, C_2, C_1B, C_2B\}, \{C_1B, C_2B\}\}$. This grouping structure ensures that the dummy variables representing a categorical variable are selected collectively, and if an interaction term is selected, the corresponding main terms are also selected. Detailed information on how to determine the grouping structure is provided in C.

We compare our method with the ℓ_1 -penalized Cox models with time-dependent covariates (CoxL, Cox LASSO) using the `glmnet` package in R. The `glmnet` package provides an implementation of the (time-dependent) Cox model using ℓ_1 regularization. We use this implementation as a baseline for comparison with our method.

The performance of the two methods was evaluated using several measures, as presented in Table S2. For each simulated dataset, these measures were calculated individually and then averaged to obtain the overall performance statistics. The weight ω_g for each group in the penalization term is set to one. We use a convergence criterion of 10^{-5} , which is based on the sum of the absolute differences between the estimates from the two steps. In the process of model selection, we compare both the *min* and *lse* rules for choosing the tuning parameter λ . The results are given in Table S3.

Our `sox` method always followed both of the rules as designed. However, Cox LASSO with the *min* rule fails to respect the categorical selection rule in 20%-40% of the cases, and it violates the strong heredity rule in 80% of the cases in certain settings, even with increased sample sizes. It is important to note that in scenario 2, Cox LASSO had a higher probability of breaking the rules. When applying the *min* rule, both methods achieved a perfect missing rate. Additionally, it is observed that `sox` converged faster than Cox LASSO. However, when applying the *lse* rule, the missing rate of `sox` converged faster compared to Cox LASSO. This confirms that `sox` had a higher chance of successfully selecting the variables that should be selected, even with a relatively small sample size.

For both methods, the false alarm rate was much worse when using the *min* rule, indicating that the methods select a significant number of noise variables. Therefore, in a low-dimensional setting, if the objective is to recover the sparsity pattern, it is advisable to avoid applying the *min* rule. However, it is worth noting that the false alarm rate of `sox` with the *lse* rule converged to 0 relatively quickly with increasing sample sizes. The MSE of `sox` was significantly smaller and converged faster compared to Cox LASSO under either rule, indicating that `sox` achieved better estimation performance. The cross-validated errors and prediction accuracy of both methods are similar across all the settings.

Overall, the simulation results verify that `sox` can more effectively recover the sparsity pattern and provide better estimation when incorporating the correct selection rules.

5.2 Interaction selection under time-dependent, high-dimensional setting

We follow the design outlined in She et al.⁴⁴ to perform interaction selection. In this model, our goal is to identify significant two-way interactions from all the potential ones while adhering to the strong heredity selection rule. We generate time-dependent predictors denoted as $X = (X^{\text{main}}, X^{\text{inter}})$. Within $X^{\text{main}} = (X_1, \dots, X_{p'})$, each main term is generated following a standard normal distribution, similar to the low-dimensional case (e.g., $B(t)$). We introduce four time-varying points, with each variable held constant for two or three time-points. Subsequently, we create $X^{\text{inter}} = (X_1 X_2, \dots, X_1 X_{p'}, X_2 X_3, \dots, X_{p'-1} X_{p'})$. The true coefficient vector is denoted as

$$\beta = (\beta_1, \dots, \beta_{p'}, \beta_{1,2}, \dots, \beta_{1,p'}, \beta_{2,3}, \dots, \beta_{p'-1,p'})^\top$$

which has a length of $p' + \binom{p'}{2}$, matching the dimension of the combined predictors in X .

We generate time-to-event outcomes using the R package `PermAlgo`⁴³. For all simulations with different combinations of n and p , we set the nine coefficients of the main terms $\beta_j, \forall j = 1, \dots, 9$ as 0.4 and the nine coefficients of interaction terms $\beta_{j,j'} = 0.3$ for $(j, j') = (1, 2), (1, 3), (1, 7), (1, 8), (1, 9), (4, 5), (4, 6), (7, 8)$ and $(7, 9)$. All other coefficients are set to zero.

To enforce the strong heredity selection rule, we define the grouping structure as follows:

$$\mathfrak{g}_1 = \{X_1, X_1 X_2, \dots, X_1 X_{p'}\}, \dots, \mathfrak{g}_{p'} = \{X_{p'}, X_1 X_{p'}, \dots, X_{p'-1} X_{p'}\}, \quad \mathfrak{g}_{p'+1} = \{X_1 X_2\}, \dots, \mathfrak{g}_{p'+\binom{p'}{2}} = \{X_{p'-1} X_{p'}\}.$$

We consider six different combinations of (n, p) with $n = (400, 800)$ and $p = p' + \binom{p'}{2} = (210, 465, 820)$, where $p' = (20, 30, 40)$ represents the number of main terms. Since `SGL` and `grpCox` do not support the time-dependent model, we only compare the performance of `sox` with the LASSO regularized Cox model (both using the *min* rule). The optimal value of λ was selected from a sequence of candidate values through 10-fold cross-validation. We also applied adaptive penalty weights to obtain debiased estimates (db). Specifically, the adaptive regularization weights were calculated as the inverse of the original `sox` or the LASSO Cox estimates $\omega_{\mathfrak{g}} = 1 / \max(|\hat{\beta}_{\mathfrak{g}}|, 10^{-16})$.

We assess selection consistency using the same metrics as in Section 5.1. The results of these evaluations are presented in Table S4. In summary, `sox` outperforms `CoxL` in several aspects. Firstly, `sox` strictly adheres to the strong heredity selection rule, which is not achieved by `CoxL`. Secondly, `sox` exhibits lower missing rates than `CoxL` when $n = 400$ and comparable missing rates when $n = 800$. Debiased `sox` has the lowest false alarm rates in most cases. This can be attributed to the enforcement of the selection rule, where the elimination of an interaction term from the model is triggered not only by the term itself but also by the absence of either of its main terms. Furthermore, `sox` demonstrates higher estimation accuracy, as evidenced by the lower mean-squared errors.

When incorporating the strong heredity selection rule, the algorithm forces the selection of the two main terms when an interaction is selected, which would increase the false alarm rate if the selected interaction term is a noisy variable. Therefore, the false alarm rate of `sox` can be slightly higher than the methods without incorporating the selection rule. However, by employing our method, we can achieve a lower missing rate and more importantly, an interpretable prediction model.

Similar conclusions can be made when the *Ise* rule is applied. The results are given in D.

5.3 Comparison with existing sparse group lasso methods

In this section, we compare `sox` with two existing packages, `SGL`⁴⁵ and `grpCox`⁴⁶, both of which implement the sparse group lasso for the time-fixed Cox model. Specifically, `grpCox` achieves within-group sparsity by utilizing a latent group LASSO approach^{47,48}.

Following Simon et al.¹⁰, we simulate a covariate matrix \mathbf{X} with dimensions $n = 100$ and $p = 200$. The columns of \mathbf{X} are independently generated from a standard Gaussian distribution. The variables X_1, \dots, X_{200} are divided into 10 groups, each containing 20 variables.

We consider three different cases of true coefficients

$$\begin{aligned} \text{Case 1:} \quad & \beta = (\beta_s^\top, 0, \dots, 0)^\top, \\ \text{Case 2:} \quad & \beta = (\beta_s^\top, \beta_s^\top, 0, \dots, 0)^\top, \\ \text{Case 3:} \quad & \beta = (\beta_s^\top, \beta_s^\top, \beta_s^\top, 0, \dots, 0)^\top, \end{aligned}$$

6 Case study: time-dependent predictor identification for time to death by any cause among patients hospitalized for atrial fibrillation

Background

Atrial fibrillation (AF) is a medical condition characterized by an irregular heartbeat. Patients with AF are at a higher risk of experiencing cardiovascular complications and mortality⁵⁰. Therefore, it is important to identify predictors that contribute to these outcomes and develop a predictive model that can help understand the disease and support clinical decision-making.

In treating AF, most patients are prescribed oral anticoagulants (OAC) for long-term management. OAC includes medications such as warfarin and direct OAC (DOAC), the latter including Dabigatran, Apixaban, and Rivaroxaban, each of which can be taken as high or low dose. However, the use of OAC in AF patients is often intermittent due to contraindications, adverse effects, and the need for surgeries⁵¹. Furthermore, the use of other medications and changes in disease conditions may vary over time among AF patients. Taking into account such time-varying information can be beneficial in identifying predictors of clinical outcomes in AF patients⁵².

Data

In this study, we utilize the `sox` method to identify significant baseline and time-varying predictors associated with the time to all-cause death among patients hospitalized for AF who initiated OAC between 2010 and 2017 in the province of Quebec, Canada. The data used in this study were obtained from a larger dataset⁵³ and represent 36,381 patients who were followed up for a period of 365 days. To ensure the validity of the analysis, we applied specific inclusion and exclusion criteria to the dataset, which are detailed in I. Among the included patients, a total of 4,384 individuals experienced the event of interest (i.e., death by any cause) during the follow-up period, accounting for approximately 12.05% of the population.

In this study, we selected a total of 24 candidate predictors based on previous research findings^{54,55,56,57} and data availability. Out of these predictors, 7 are baseline (time-invariant) covariates. The baseline covariates include age, sex, medical scores, comorbidities (eight conditions), OAC use information, concomitant medication use (four drugs), and the interactions between each concomitant medication and DOAC. Additionally, we define five time-dependent indicator covariates to capture OAC use: DOAC, Apixaban, Dabigatran, OAC, and High-dose-DOAC.

The definitions and summary statistics for the covariates are provided in J and K, respectively. It is worth noting that the time-dependent covariates, especially those related to OAC use, exhibited significant changes over time. This highlights the importance of considering the time-varying nature of these covariates, as neglecting their changes may introduce substantial bias in covariates selection and coefficient estimation.

Analysis

To assess the associations between the covariates and the time to the event of interest, we conduct both univariate and multivariate time-dependent Cox models. The crude hazard ratios from the univariate models and the adjusted hazard ratios from the multivariate models, along with their corresponding 95% confidence intervals, are presented in L.

For this data analysis, we establish selection rules (including strong heredity and the rules for coefficients interpretability) to ensure the interpretability of the model. The specific selection rules are outlined in Table S6. It aims to capture the following associations: 1) The use of OAC versus non-use; 2) The use of DOAC compared to warfarin; 3) The use of Apixaban compared to Rivaroxaban; 4) The use of Dabigatran compared to Rivaroxaban; 5) The use of high-dose-DOAC compared to low-dose-DOAC; 6) The simultaneous use of concomitant medication and DOAC.

The selection rules ensure that the aforementioned comparisons are estimable and correspond to the coefficients of the selected variables if selected. Further explanation and rationale for these selection rules can be found in M. To respect these selection rules simultaneously, we identified the appropriate graph-structured grouping structure, which is provided in N, following the approach described in^{20,58}.

Results

First, we applied both the `sox` method and Cox LASSO to select variables from the data. We then used the unpenalized time-dependent Cox model to estimate the hazard ratios for the selected covariates. Additionally, we report the estimates with 95% confidence intervals when all the covariates are included in the model. The results are given in Table S7. Our proposed method, `sox`, identified 15 predictors that are associated with the outcome. Comparing Cox LASSO with `sox`, we observe the following differences: 1) DOAC was not selected by Cox LASSO, which affects the interpretation of the coefficient of Apixaban; 2) the interaction of DOAC and Statin was selected without Statin in Cox LASSO, violating the strong heredity assumption; 3)

predictors such as High-dose-DOAC and Beta-Blockers were not selected by Cox LASSO. Additionally, our method achieves a slightly higher concordance index compared to the unstructured penalization, though slightly lower than the full model. These results demonstrate the advantages of utilizing `sox` over Cox LASSO, highlighting the benefits of incorporating prior knowledge about the underlying structure of the data. To further illustrate the results, we visualize the impact of time-dependent covariates on the survival probability. See more details in O.

7 Discussion

In both low and high-dimension settings, incorporating a priori knowledge of covariate structures can achieve robust and interpretable models. In survival models, especially when the covariates and coefficients are time-dependent, no clear guidance and methods are available for the incorporation of such prior information. In this paper, we introduced `sox`, a novel structured sparsity-inducing penalty for the time-dependent Cox model. The method can accommodate a wide range of a priori knowledge about the data structure in the form of restrictions on covariate inclusion. We empirically showed that incorporating correct selection rules can improve model selection performance and accuracy of estimation. The developed algorithm converges fast and is able to handle high-dimensional data, which can be implemented in the developed R package. Through examples, simulations, and the case study, we also explored how to set appropriate selection rules and the corresponding grouping structures for the developed method in practice, which provided users with guidance on the implementation of the methods in their own application.

We would also like to emphasize that our work primarily focuses on scenarios where practitioners have prior knowledge of the definition of each variable and its relationship with others, aiming to produce an interpretable prediction model. For instance, variables may be defined as interactions of other variables to ensure the interpretability of the resulting coefficients, necessitating the use of strong heredity (as demonstrated in various examples in Web Appendix A and the case study).

In practical situations where the definition of a variable or its relationship with other variables is unclear, we recommend not including the variable in a selection rule or performing sensitivity analysis. In such cases, it is prudent to use more conservative methods like the LASSO. Incorporating uncertain or incorrect selection rules can potentially degrade the performance of the resulting model.

There are several avenues for future work. For instance, one could relax the assumption that the hazard is dependent on the current value of the covariates, assume event times follow a parametric distribution by using accelerated failure time models⁵⁹, generalize to different penalty types (for example, minimax concave penalty,⁶⁰ or smoothly clipped absolute deviation⁶¹), and investigate the impact of applying different weighting schemes. In addition, it would be beneficial to integrate structured variable selection into causal inference, especially when the confounders or effect modifiers are high-dimensional^{62,63,64,65,66,67}.

Software

The R package developed for the proposed method is available at <https://cran.r-project.org/package=sox>. The R code for simulation is available at https://github.com/Guanbo-W/sox_sim.

Supplementary Material

The reader is referred to the on-line Supplementary Materials for technical appendices.

Acknowledgments

We would like to thank the Régie de l'Assurance Maladie du Québec (RAMQ) and Ministry of Health and Social Services (MSSS) (Quebec, Canada) for providing assistance in handling the data and the Commission d'accès à l'information for authorizing the study. G. Wang is supported by the Fonds de Recherche du Québec Santé (FRQS-272161). AY. Yang is supported by the Natural Sciences and Engineering Research Council of Canada (NSERC) Discovery Grant RGPIN-2016-05174 and Fonds

de Recherche du Québec Nature et Technologies Team Grant (FRQNT-327788). ME. Schnitzer is supported by a Canadian Institutes of Health Research Canada (CIHR) Research Chair tier 2 and an NSERC Discovery Grant. RW. Platt is supported by CIHR Foundation Grant (FDN-143297). The study was supported by the Heart and Stroke Foundation of Canada (G-17-0018326) and the Réseau Québécois de Recherche sur les Médicaments (RQRM). Please refer to the following <https://www.heartandstroke.ca/> and <http://www.frqs.gouv.qc.ca/en/>. *Conflict of Interest*: None declared.

References

1. Reid N, Cox D. *Analysis of survival data*. Chapman and Hall/CRC . 2018.
2. Holcomb JB, others . The prospective, observational, multicenter, major trauma transfusion (PROMMTT) study: comparative effectiveness of a time-varying treatment with competing risks. *JAMA surgery* 2013; 148(2): 127–136.
3. Weisz G, others . Ranolazine in patients with incomplete revascularisation after percutaneous coronary intervention (RIVER-PCI): a multicentre, randomised, double-blind, placebo-controlled trial. *The Lancet* 2016; 387(10014): 136–145.
4. Huang J, Sun T, Ying Z, Yu Y, Zhang CH. Oracle inequalities for the lasso in the Cox model. *Annals of statistics* 2013; 41(3): 1142.
5. Fan J, Li R. Variable selection for Cox’s proportional hazards model and frailty model. *Annals of Statistics* 2002: 74–99.
6. Beretta A, Heuchenne C. Variable selection in proportional hazards cure model with time-varying covariates, application to US bank failures. *Journal of Applied Statistics* 2019; 46(9): 1529–1549.
7. Yan J, Huang J. Model selection for Cox models with time-varying coefficients. *Biometrics* 2012; 68(2): 419–428.
8. Lim M, Hastie T. Learning interactions via hierarchical group-lasso regularization. *Journal of Computational and Graphical Statistics* 2015; 24(3): 627–654.
9. Wang L, Shen J, Thall PF. A modified adaptive Lasso for identifying interactions in the Cox model with the heredity constraint. *Statistics & probability letters* 2014; 93: 126–133.
10. Simon N, Friedman J, Hastie T, Tibshirani R. A sparse-group lasso. *Journal of computational and graphical statistics* 2013; 22(2): 231–245.
11. Wang S, Nan B, Zhu N, Zhu J. Hierarchically penalized Cox regression with grouped variables. *Biometrika* 2009; 96(2): 307–322.
12. Dang X, Huang S, Qian X. Penalized cox’s proportional hazards model for high-dimensional survival data with grouped predictors. *Statistics and Computing* 2021; 31: 1–27.
13. Obozinski G, Jacob L, Vert JP. Group lasso with overlaps: the latent group lasso approach. *arXiv preprint arXiv:1110.0413* 2011.
14. Villa S, Rosasco L, Mosci S, Verri A. Proximal methods for the latent group lasso penalty. *Computational Optimization and Applications* 2014; 58: 381–407.
15. Jenatton R, Audibert JY, Bach F. Structured variable selection with sparsity-inducing norms. *The Journal of Machine Learning Research* 2011; 12: 2777–2824.
16. Lian Y, Wang G, Yang AY, et al. *sox: Structured Learning in Time-Dependent Cox Models*. 2023. R package version 1.0.
17. Breslow N. Covariance analysis of censored survival data. *Biometrics* 1974: 89–99.
18. Kim J, Sohn I, Jung SH, Kim S, Park C. Analysis of survival data with group lasso. *Communications in Statistics-Simulation and Computation* 2012; 41(9): 1593–1605.
19. Yan X, Bien J, others . Hierarchical sparse modeling: A choice of two group lasso formulations. *Statistical Science* 2017; 32(4): 531–560.
20. Wang G, Schnitzer ME, Chen T, Wang R, Platt RW. A general framework for formulating structured variable selection. *arXiv* 2023.
21. Mairal J, Jenatton R, Obozinski G, Bach F. Convex and Network Flow Optimization for Structured Sparsity.. *Journal of Machine Learning Research* 2011; 12(9).
22. Boyd S, Vandenberghe L. *Convex optimization*. Cambridge university press . 2004.
23. Moreau JJ. Fonctions convexes duales et points proximaux dans un espace hilbertien. *Comptes rendus hebdomadaires des séances de l’Académie des sciences* 1962; 255: 2897–2899.
24. Combettes PL, Pesquet JC. Proximal splitting methods in signal processing. In: Springer. 2011 (pp. 185–212).

25. Bach F. Structured sparsity-inducing norms through submodular functions. *Advances in Neural Information Processing Systems* 2010; 23.
26. Beck A, Teboulle M. A fast iterative shrinkage-thresholding algorithm for linear inverse problems. *SIAM journal on imaging sciences* 2009; 2(1): 183–202.
27. Nesterov Y. Gradient methods for minimizing composite objective function. CORE Discussion Papers 2007076, Université catholique de Louvain, Center for Operations Research and Econometrics (CORE); 2007.
28. Beck A. *First-order methods in optimization*. 25. SIAM . 2017.
29. Jenatton R, Mairal J, Obozinski G, Bach F. Proximal methods for hierarchical sparse coding. *Journal of Machine Learning Research* 2011; 12(Jul): 2297–2334.
30. Bertsekas D. *Network optimization: continuous and discrete models*. 8. Athena Scientific . 1998.
31. Ford LR, Fulkerson DR. Maximal flow through a network. *Canadian journal of Mathematics* 1956; 8: 399–404.
32. Babenko M, Goldberg AV. Experimental evaluation of a parametric flow algorithm. *Technical Report MSR-TR-2006-77* 2006.
33. Mairal J, Bach F, Ponce J. Sparse modeling for image and vision processing. *arXiv preprint arXiv:1411.3230* 2014.
34. Therneau TM. *A Package for Survival Analysis in R*. 2021. R package version 3.2-10.
35. Friedman J, Hastie T, Tibshirani R. Regularization paths for generalized linear models via coordinate descent. *Journal of statistical software* 2010; 33(1): 1.
36. Simon N, Friedman J, Hastie T, Tibshirani R. Regularization paths for Cox’s proportional hazards model via coordinate descent. *Journal of statistical software* 2011; 39(5): 1.
37. Goldberg AV, Tarjan RE. A new approach to the maximum-flow problem. *Journal of the ACM (JACM)* 1988; 35(4): 921–940.
38. Cherkassky BV, Goldberg AV. On implementing the push—relabel method for the maximum flow problem. *Algorithmica* 1997; 19(4): 390–410.
39. Bertsekas DP. Nonlinear programming. *Journal of the Operational Research Society* 1997; 48(3): 334–334.
40. Chen Y, Yang Y. The One Standard Error Rule for Model Selection: Does It Work?. *Stats* 2021; 4(4): 868–892.
41. Zhang Z, others . Time-varying covariates and coefficients in Cox regression models. *Annals of translational medicine* 2018; 6(7).
42. R Core Team . *R: A Language and Environment for Statistical Computing*. R Foundation for Statistical Computing; Vienna, Austria: 2021.
43. Sylvestre MP, Evans T, MacKenzie T, Abrahamowicz M. *PermAlgo: Permutational algorithm to generate event times conditional on a covariate matrix including time-dependent covariates*. 2010. R package version 1.1.
44. She Y, Wang Z, Jiang H. Group regularized estimation under structural hierarchy. *Journal of the American Statistical Association* 2018; 113(521): 445–454.
45. Simon N, Friedman J, Hastie T, Tibshirani R. *SGL: Fit a GLM (or Cox Model) with a Combination of Lasso and Group Lasso Regularization*. 2019. R package version 1.3.
46. Dang X. *grpCox: Penalized Cox Model for High-Dimensional Data with Grouped Predictors*. 2020. R package version 1.0.1.
47. Jacob L, Obozinski G, Vert JP. Group lasso with overlap and graph lasso. In: ; 2009: 433–440.
48. Obozinski G, Jacob L, Vert JP. Group lasso with overlaps: the latent group lasso approach. *arXiv preprint arXiv:1110.0413* 2011.
49. Kropko J, Harden J. *coxed: Duration-Based Quantities of Interest for the Cox Proportional Hazards Model*. 2020. R package version 0.3.3.
50. Lip GY, Tse HF. Management of atrial fibrillation. *The Lancet* 2007; 370(9587): 604–618.
51. Angiolillo DJ, others . Antithrombotic therapy in patients with atrial fibrillation treated with oral anticoagulation undergoing percutaneous coronary intervention: a North American perspective: 2021 update. *Circulation* 2021; 143(6): 583–596.
52. Claxton JS, others . A new model to predict major bleeding in patients with atrial fibrillation using warfarin or direct oral anticoagulants. *PloS one* 2018; 13(9): e0203599.
53. Perreault S, others . Oral anticoagulant prescription trends, profile use, and determinants of adherence in patients with atrial fibrillation. *Pharmacotherapy: The Journal of Human Pharmacology and Drug Therapy* 2020; 40(1): 40–54.
54. Fauchier L, others . Cause of death in patients with atrial fibrillation admitted to French hospitals in 2012: a nationwide database study. *Open Heart* 2015; 2(1): e000290.

55. Fauchier L, others . Causes of death and influencing factors in patients with atrial fibrillation. *The American journal of medicine* 2016; 129(12): 1278–1287.
56. Lee E, others . Mortality and causes of death in patients with atrial fibrillation: a nationwide population-based study. *PLoS One* 2018; 13(12): e0209687.
57. Harb SC, others . CHA2DS2-VASc score stratifies mortality risk in patients with and without atrial fibrillation. *Open Heart* 2021; 8(2): e001794.
58. Wang G, Perreault S, Platt RW, Wang R, Dorais M, Schnitzer ME. Integrating complex selection rules into the latent overlapping group Lasso for constructing coherent prediction models. *arXiv preprint arXiv:2206.05337* 2023.
59. Kalbfleisch JD, Prentice RL. *The statistical analysis of failure time data*. 360. John Wiley & Sons . 2011.
60. Zhang CH. Nearly unbiased variable selection under minimax concave penalty. *The Annals of statistics* 2010; 38(2): 894–942.
61. Fan J, Li R. Variable selection via nonconcave penalized likelihood and its oracle properties. *Journal of the American statistical Association* 2001; 96(456): 1348–1360.
62. Siddique AA, Schnitzer ME, Bahamyirou A, et al. Causal inference with multiple concurrent medications: A comparison of methods and an application in multidrug-resistant tuberculosis. *Statistical methods in medical research* 2019; 28(12): 3534–3549.
63. Wang G, Schnitzer ME, Menzies D, Viiklepp P, Holtz TH, Benedetti A. Estimating treatment importance in multidrug-resistant tuberculosis using Targeted Learning: An observational individual patient data network meta-analysis. *Biometrics* 2020; 76(3): 1007–1016.
64. Liu Y, Schnitzer ME, Wang G, et al. Modeling treatment effect modification in multidrug-resistant tuberculosis in an individual patient data meta-analysis. *Statistical methods in medical research* 2022; 31(4): 689–705.
65. Wang G, Poulin-Costello M, Pang H, et al. Evaluating hybrid controls methodology in early-phase oncology trials: A simulation study based on the MORPHEUS-UC trial. *Pharmaceutical Statistics* 2023; n/a(n/a). doi: <https://doi.org/10.1002/pst.2336>
66. Wang G. Review 1: "Antibiotic Prescribing in Remote Versus Face-to-Face Consultations for Acute Respiratory Infections in English Primary Care: An Observational Study Using TMLE". *Rapid Reviews Infectious Diseases* 2023.
67. Bouchard A, Bourdeau F, Roger J, et al. Predictive Factors of Detectable Viral Load in HIV-Infected Patients. *AIDS Research and Human Retroviruses* 2022; 38(7): 552–560.
68. Haris A, Witten D, Simon N. Convex Modeling of Interactions With Strong Heredity. *Journal of Computational and Graphical Statistics* 2016; 25(4): 981–1004. doi: 10.1080/10618600.2015.1067217
69. Reisberg B, others . The Global Deterioration Scale for assessment of primary degenerative dementia.. *The American journal of psychiatry* 1982.
70. Zhai T, Gu H, Yang Y. Cox regression based modeling of functional connectivity and treatment outcome for relapse prediction and disease subtyping in substance use disorder. *Frontiers in Neuroscience* 2021; 15: 768602.
71. Lee YB, others . Sparse SPM: Group Sparse-dictionary learning in SPM framework for resting-state functional connectivity MRI analysis. *NeuroImage* 2016; 125: 1032–1045.
72. Chklovskii DB, Koulakov AA. Maps in the brain: what can we learn from them?. *Annu. Rev. Neurosci.* 2004; 27: 369–392.
73. Ward Jr JH. Hierarchical grouping to optimize an objective function. *Journal of the American statistical association* 1963; 58(301): 236–244.
74. Jenatton R, Gramfort A, Michel V, et al. Multiscale mining of fMRI data with hierarchical structured sparsity. *SIAM Journal on Imaging Sciences* 2012; 5(3): 835–856.

Type	From	To	Flow f	Capacity c
1	s_1	$\mathfrak{g}_k \in \mathbb{G}$	$\sum_{X_j \in \mathbb{V}} \sum_{\mathfrak{g} \in \mathbb{G}} \xi_{ \mathfrak{g}}^j$	$\lambda \omega_{\mathfrak{g}}$
2	\mathfrak{g}_k	$X_j \in \mathfrak{g}_k$	$\xi_{ \mathfrak{g}}^j$	∞
3	$X_j \in \mathbb{V}$	s_2	$(\sum_{\mathfrak{g} \in \mathbb{G}} \xi_{ \mathfrak{g}}^j)_{X_j \in \mathbb{V}}$	∞

Table S1 Corresponding inputs of the max flow algorithm.

#	Measurements
(1)	Missing rate (MR): the percentage of variables not selected among the true predictors.
(2)	False alarm rate (FAR) : the percentage of selected variables among the noise variables.
(3)	Rule 1 Satisfaction (R1S): whether the selected model satisfied strong heredity.
(4)	Rule 2 Satisfaction (R2S): whether the resulting selected model satisfied selection rule 2, that dummy indicators of the same variable are always selected together.
(5)	C index (RCI): the C index of the selected model.
(6)	Mean-squared error (MSE): the mean of the squared differences between each coefficient in the data generating mechanism and its estimate, i.e., the ℓ_2 -norm of the difference between the coefficient vector and its estimate.
(7)	Cross-validated error (CV-E): the cross-validated error defined in Section 4.

Table S2 Measures of comparison in the the simulation studies

Scenario	1 (A≠0)				2 (A, B, AB≠0)			
	sox.1se	sox.min	CoxL.1se	CoxL.min	sox.1se	sox.min	CoxL.1se	CoxL.min
<i>N</i> = 100								
MR	0.82	0.02	0.85	0.26	0.08	0.00	0.41	0.16
FAR	0.02	0.65	0.03	0.40	0.04	0.53	0.06	0.49
R1S	1.00	1.00	0.88	0.70	1.00	1.00	0.84	0.72
R2S	1.00	1.00	0.75	0.38	1.00	1.00	0.39	0.35
RCI	0.53	0.67	0.54	0.64	0.91	0.92	0.91	0.92
MSE	0.24	0.06	0.27	0.14	0.27	0.10	0.41	0.30
CV-E	6.87	6.74	6.68	6.59	4.70	4.36	4.74	4.33
<i>N</i> = 500								
MR	0.12	0.00	0.32	0.00	0.00	0.00	0.36	0.04
FAR	0.02	0.70	0.01	0.54	0.00	0.15	0.05	0.59
R1S	1.00	1.00	0.90	0.57	1.00	1.00	0.94	0.78
R2S	1.00	1.00	0.79	0.22	1.00	1.00	0.45	0.62
RCI	0.60	0.63	0.58	0.63	0.91	0.91	0.91	0.91
MSE	0.14	0.02	0.22	0.03	0.14	0.04	0.31	0.07
CV-E	6.79	6.70	6.81	6.68	4.38	4.26	4.40	4.26
<i>N</i> = 1000								
MR	0.00	0.00	0.04	0.00	0.00	0.00	0.20	0.02
FAR	0.02	0.73	0.02	0.58	0.00	0.08	0.04	0.66
R1S	1.00	1.00	0.97	0.70	1.00	1.00	0.90	0.82
R2S	1.00	1.00	0.94	0.31	1.00	1.00	0.53	0.65
RCI	0.61	0.62	0.60	0.62	0.91	0.91	0.91	0.91
MSE	0.10	0.01	0.15	0.02	0.12	0.02	0.29	0.08
CV-E	6.76	6.68	6.76	6.67	4.33	4.25	4.36	4.24
<i>N</i> = 2000								
MR	0.00	0.00	0.00	0.00	0.00	0.00	0.08	0.00
FAR	0.00	0.06	0.00	0.54	0.00	0.00	0.04	0.57
R1S	1.00	1.00	1.00	0.60	1.00	1.00	0.93	0.76
R2S	1.00	1.00	0.99	0.20	1.00	1.00	0.79	0.57
RCI	0.61	0.61	0.61	0.61	0.91	0.91	0.91	0.91
MSE	0.06	0.00	0.10	0.01	0.12	0.05	0.23	0.01
CV-E	6.71	6.66	6.72	6.66	4.30	4.23	4.31	4.23

Table S3 Simulation results of Section 5.1. Cox LASSO: unstructured ℓ_1 penalty (glmnet with cox); sox: our method; 1se: applying the 1se rule; min: applying the min rule. MR: Missing rate, FAR: False alarm rate, R1S: Rule 1 Satisfaction, R2S: Rule 2 Satisfaction, RCI: the C index of the model with the selected variables, MSE: Mean-squared error, CV-E: cross-validated error

Method	sox	sox.db	CoxL	CoxL.db	sox	sox.db	CoxL	CoxL.db
$p = 210$		$n = 400$			$n = 800$			
MR	0.04	0.06	0.05	0.07	0.02	0.04	0.01	0.01
FAR	0.27	0.11	0.21	0.18	0.14	0.03	0.20	0.19
R1S	1.00	1.00	0.87	0.89	1.00	1.00	0.88	0.89
RCI	0.88	0.86	0.89	0.88	0.85	0.83	0.85	0.85
MSE*	4.97	3.91	5.97	4.86	4.37	3.88	5.21	4.11
CV-E	1.74	1.70	1.76	1.60	1.68	1.67	1.69	1.61
$p = 465$		$n = 400$			$n = 800$			
MR	0.06	0.08	0.11	0.12	0.01	0.04	0.01	0.01
FAR	0.17	0.10	0.11	0.10	0.12	0.04	0.12	0.11
R1S	1.00	1.00	0.91	0.92	1.00	1.00	0.90	0.91
RCI	0.91	0.87	0.91	0.91	0.86	0.84	0.87	0.87
MSE*	2.45	1.77	2.95	2.50	2.63	2.55	3.14	2.58
CV-E	1.76	1.66	1.79	1.52	2.04	1.66	2.46	1.94
$p = 820$		$n = 400$			$n = 800$			
MR	0.05	0.07	0.14	0.15	0.02	0.04	0.03	0.03
FAR	0.14	0.08	0.07	0.06	0.10	0.05	0.08	0.08
R1S	1.00	1.00	0.94	0.94	1.00	1.00	0.93	0.93
RCI	0.93	0.90	0.92	0.92	0.88	0.86	0.89	0.89
MSE*	1.45	0.98	1.78	1.57	1.19	0.92	1.47	1.21
CV-E	1.79	1.67	1.84	1.48	1.70	1.67	1.73	1.53

Table S4 Simulation results of Section 5.2. In the tuning process, “lambda.min” is used. Results are averaged over 20 independent replications. CoxL: unstructured ℓ_1 penalty (glmnet with "cox" family); sox: our method; .db: with additional debiasing procedure. JDR: joint detection rate, MR: missing rate, FAR: false alarm rate, R1S: rule 1 satisfaction, RCI: the C index of the model with the selected variables, MSE: mean-squared error (*values are multiplied by 10^{-3}), CV-E: cross-validated error.

	sox	SGL	grpCox	sox	SGL	grpCox	sox	SGL	grpCox
	Case 1			Case 2			Case 3		
MR	0.27	0.31	0.71	0.34	0.30	0.79	0.36	0.46	0.82
FAR	0.13	0.12	0.02	0.17	0.18	0.02	0.20	0.16	0.02
MSE*	2.04	2.02	2.21	4.38	4.19	4.77	7.28	7.25	7.49

MSE: $\|\beta - \hat{\beta}\|_2^2/p$, values are multiplied by 10^{-3} .

Table S5 Simulation results of Section 5.3. In the tuning process, “lambda.min” is used. Results are averaged over 20 independent replications. sox: our method, SGL the sparse group LASSO, grpCox: the latent overlapping group LASSO.

#	Selection rule
1	If Apixaban is selected, then select DOAC
2	If Dabigatran is selected, then select DOAC
3	If DOAC is selected, then select OAC
4	If High-dose-DOAC is selected, then select DOAC
5...8	If the interaction of DOAC and a concomitant medication is selected, then both DOAC and the concomitant medication are selected.

Table S6 Selection rules for the case study

Covariate	sox.refit	CoxL.refit	Cox
C-Index	0.8034	0.7991	0.8077
Age (≥ 75)	1.84	1.80	1.85 (1.70, 2.03)
Sex(female/male)	-	-	0.96 (0.90, 1.03)
Comorbidities/Medical score			
CHA ₂ DS ₂ VAS _c (≥ 3)	0.84	-	0.90 (0.80, 1.02)
Diabetes	-	-	1.08 (1.01, 1.15)
COPD/asthma	1.51	1.49	1.49 (1.41, 1.59)
Hypertension	-	-	0.89 (0.81, 0.97)
Malignant cancer	1.56	1.58	1.55 (1.46, 1.65)
Stroke	-	-	0.95 (0.88, 1.02)
Chronic kidney disease	2.40	2.34	2.39 (2.23, 2.55)
Heart disease	2.55	2.36	2.56 (2.31, 2.83)
Major bleeding	1.71	1.69	1.72 (1.61, 1.83)
OAC use			
DOAC	0.89	-	1.04 (0.76, 1.44)
Apixaban	0.94	0.94	0.86 (0.67, 1.12)
Dabigatran	-	-	0.80 (0.55, 1.17)
OAC	0.17	0.16	0.17 (0.15, 0.19)
High-dose-DOAC	0.91	-	0.87 (0.69, 1.11)
Concomitant medication use			
Antiplatelets	-	-	1.10 (1.03, 1.19)
NSAIDs	-	-	1.58 (1.34, 1.86)
Statin	0.65	-	0.63 (0.59, 0.67)
Beta-Blockers	1.04	-	1.03 (0.97, 1.10)
Potential drug-drug interaction			
DOAC: Antiplatelets	-	-	0.67 (0.50, 0.90)
DOAC: NSAIDs	-	-	0.76 (0.43, 1.37)
DOAC: Statin	1.05	0.66	1.15 (0.90, 1.48)
DOAC: Beta-Blockers	0.83	-	0.86 (0.68, 1.10)

Table S7 The estimated hazard ratios and 95% confidence intervals of each covariate from various methods. CoxL.refit: unstructured ℓ_1 penalty; sox.refit: our method; Cox: the standard time dependent-Cox model with all covariates included; C-Index: concordance index

How to cite this article: G. Wang, Y. Lian, AY. Yang, RW. Platt, R. Wang, S. Perreault, M. Dorais, and ME. Schnitzer (xxxx), Structured Learning in Time-dependent Cox Models, *xx*, *xx*.

Appendix

Supplementary materials

A Examples of various types of selection rules and grouping structures

Example A.1 (Coefficients interpretability). Consider a cohort study in which patients intermittently receive a drug (treatment) at different dose levels. The objective is to investigate the association between dose level and time-to-event. Let $X_1(t)$ and $X_2(t)$ represent indicators for the patient receiving treatment (either high or low dose) at time t and receiving the high dose treatment, respectively. A crucial selection rule in this scenario is “if $X_2(t)$ is selected, then $X_1(t)$ must also be selected”. This is because if $X_2(t)$ is selected without $X_1(t)$, then the coefficients of $X_2(t)$ would be the contrast between taking high-dose treatment versus taking low-dose treatment combined with not taking the treatment, which is not of interest. Incorporating such selection rules guarantees the interpretability of the selected model’s coefficients. To satisfy this selection rule, the grouping structure \mathbb{G} is specified as $\{\{X_2(t)\}, \{X_1(t), X_2(t)\}\}$. It is worth noting that even this simple selection rule necessitates an overlapping grouping structure.

Example A.2 (Strong heredity). As mentioned earlier, caution is required when dealing with interaction terms in variable selection. Consider a study involving covariates $X_1(t)$, $X_2(t)$ and their interaction $X_3(t) = X_1(t) \times X_2(t)$. The strong heredity⁸ states that “If the interaction term is selected, then all its main terms must also be selected”. We specify the grouping structure as $\mathbb{G} = \{\{X_3(t)\}, \{X_1(t), X_3(t)\}, \{X_2(t), X_3(t)\}\}$. Incorporating such selection rules can enhance the interpretability of the model, improve statistical power, and simplify experimental designs⁶⁸. In our simulation studies, we present additional examples of grouping structures for more complex scenarios. For instance, in Section 5.1, we demonstrate the grouping structure for the case involving interactions between two categorical variables and a continuous variable. In Section ??, we showcase the strategy for setting the grouping structure when high-dimensional main terms and interactions are included.

Example A.3 (Incorporating temporal structure). In studies involving patients with dementia, it is common to categorize them into four phases: mild, moderate, moderately severe, and severe cognitive decline⁶⁹. Consider a cohort study focusing on patients diagnosed with mild cognitive decline and examining the association between blood pressure $X(t)$ at each phase and the time to severe cognitive decline. We define T_1 as the time of diagnosis for moderate cognitive decline and T_2 as the time for moderately severe cognitive decline. To capture the temporal aspect, we include the time-dependent covariates $Z_1(t) = I(t < T_1)X(t)$, $Z_2(t) = I(T_1 \leq t < T_2)X(t)$ and $Z_3(t) = I(t \geq T_2)X(t)$ in the Cox model. Suppose we have a priori knowledge that if the blood pressure in a previous phase is associated with the outcome, the blood pressure in the later phase should also be associated. This implies the following selection rules: “if $Z_1(t)$ is selected, then $Z_2(t)$ and $Z_3(t)$ should also be selected” and “if $Z_2(t)$ is selected, then $Z_3(t)$ should be selected”. By incorporating such selection rules, we can accommodate the temporal structure of the time-dependent covariate. The corresponding grouping structure is $\mathbb{G} = \{\{Z_1(t)\}, \{Z_1(t), Z_2(t)\}, \{Z_1(t), Z_2(t), Z_3(t)\}\}$. This example illustrates the use of step functions to model time-dependent associations.

More flexibly, consider the Cox model with both time-dependent covariates and coefficients, $h\{t|\mathbf{X}(t)\} = h_0(t) \cdot \exp\{\mathbf{X}(t)^\top \boldsymbol{\beta}(t)\}$, where $\boldsymbol{\beta}(t) = \{\beta_1(t), \dots, \beta_j(t)\}^\top$ with $\beta_j(t) = \sum_{m=1}^M \theta_{j,m} \phi_m(t)$, for $j = 1, \dots, p$. Rewriting, we have: $h\{t|\mathbf{Z}(t)\} = h_0(t) \cdot \exp\{\mathbf{Z}(t)^\top \boldsymbol{\theta}\}$, where $Z_{j,m}(t) = X_j(t)\phi_m(t)$, e.g.,

$$\mathbf{Z}(t) = \underbrace{(X_1(t)\phi_1(t), \dots, X_1(t)\phi_M(t), \dots, X_p(t)\phi_1(t), \dots, X_p(t)\phi_M(t))^\top}_{\mathbf{Z}_{1,\cdot}(t)}, \dots, \underbrace{}_{\mathbf{Z}_{p,\cdot}(t)}$$

which has $p \times M$ elements. Thus, in the context of predictor identification, selecting X_j is equivalent to selecting $\mathbf{Z}_{j,\cdot}(t)$. In the context of estimation, estimating $\boldsymbol{\beta}(t)$ equates to estimating the $p \times M$ length vector $\boldsymbol{\theta} = (\boldsymbol{\theta}_{1,\cdot}, \dots, \boldsymbol{\theta}_{p,\cdot})$, where $\boldsymbol{\theta}_{j,\cdot} = \{\theta_{j,1}, \dots, \theta_{j,M}\}$. Suppose the selection rule to be respected is “all the basis functions related to one variable should be selected collectively” or “ $\mathbf{Z}_{j,\cdot}(t) = \{Z_{j,1}(t), \dots, Z_{j,M}(t)\}, \forall j = 1, \dots, p$ should be selected collectively”. By incorporating such selection

rules, we can avoid the selection discrepancy among basis functions while accommodating the time-dependent coefficient feature in Cox models. We can define $\mathbb{V} = \{Z_{j,m}(t), j = 1, \dots, p, m = 1 \dots, M\}$ and $\mathbb{G} = \{Z_j(t), j = 1 \dots, p\}$, and the selection rule can be respected.

Example A.4 (Incorporating spatial structure). Suppose that high-dimensional voxel signals over time in patients' brains are collected in functional magnetic resonance imaging (fMRI) data. The goal is to identify the regions (of voxels) and individual voxels associated with the time to cocaine relapse⁷⁰ or Alzheimer's disease progression⁷¹. Variable selection conducted to analyze such data should be informed by the three-dimensional grid structure (such as localized clusters on the brain)⁷². Here we take a simplified example for illustration. Suppose there are three contiguous voxels; the intensities of the signals are denoted $X_1(t)$, $X_2(t)$, and $X_3(t)$. Consider the case where two parcels (clusters) $\{X_1(t), X_2(t)\}$ and $\{X_1(t), X_2(t), X_3(t)\}$ are hierarchically constructed⁷³, in which only neighboring voxels can be merged together. Larger parcels can be regarded as potential regions of interest. To incorporate such a structure, we first define $X_4(t)$ and $X_5(t)$ as the average of the two parcels. Then we set selection rules as "if either $X_1(t)$ or $X_2(t)$ is selected, then select $X_4(t)$ ", and "if either $X_3(t)$ or $X_4(t)$ is selected, then select $X_5(t)$ " to encode the hierarchy and promote the parcel selection⁷⁴. The corresponding \mathbb{G} is $\{\{X_1(t)\}, \{X_2(t)\}, \{X_3(t)\}, \{X_1(t), X_2(t), X_4(t)\}, \{X_1(t), X_2(t), X_3(t), X_4(t), X_5(t)\}\}$. The above example represents the case where two parcels are nested. Incorporating more complex structures, such as multiple overlapped parcels nesting in different larger parcels, is also possible.

Example A.5 (Tree and directed acyclic graph grouping structures). In certain real-world scenarios, more complex structures of covariates, such as trees²⁹ and directed acyclic graphs¹⁵, can be incorporated into variable selection. These structures allow for more intricate relationships among variables to be taken into account. For example, in our model, covariates can be represented as nodes in a tree, and users can specify that a variable is selected only if all its ancestors in the tree are already selected. Moreover, the framework can be further extended to include directed cyclic graphs, which have been found useful in hierarchical variable selection. These enhancements provide additional flexibility in capturing complex relationships among variables.

B Steps of computeFlow

Table B1 shows the steps of computeFlow.

Step	Details
Projection step	solve a relaxed version of (S4) to calculate γ , which is the lower bound of $\frac{1}{2t} \left\ \{\tilde{\beta} - t \nabla f(\tilde{\beta})\} - \gamma \right\ _2^2$, and also satisfies $\sum_j \gamma_j \leq \lambda \sum_{g \in \mathbb{G}} \omega_{ g }$. The value of γ is the projection of the vectors $\xi_{ g }^j$.
Updating step	update $(\sum_{g \in \mathbb{G}} \xi_{ g }^j)_{X_j \in \mathbb{V}}$ by maximizing $\sum_{X_j \in \mathbb{V}} \sum_{g \in \mathbb{G}} \xi_{ g }^j$, while keeping $\sum_{X_j \in g} \xi_{ g }^j \leq \lambda \omega_g$. By doing so, we can ensure that the constraint in (S4) holds. This can be done by the max flow algorithm. Details of the implementation can be found in Section 4.
Recursion step/divide and conquer	According to the mini-cut theorems ³¹ , define $\mathbb{V}^* = \{X_j \in \mathbb{V} : \sum_{g \in \mathbb{G}} \xi_{ g }^j = \gamma_j\}$, and $\mathbb{G}^* = \{g \in \mathbb{G} : \sum_{X_j \in g} \xi_{ g }^j < \lambda \omega_g\}$. Then apply steps 1 and 2 to $(\mathbb{V}^*, \mathbb{G}^*)$ and their respective complements until $(\sum_{g \in \mathbb{G}} \xi_{ g }^j)_{X_j \in \mathbb{V}}$ (obtained from step 2) matches γ (obtained from step 1).

Table B1 Steps of computeFlow

C Grouping structure identification in the simulation

The developed methods (similar to the overlapping group Lasso in²⁰) can enforce a number of groups of variable coefficients to be 0 with a certain level of penalization. The remaining variables are said to be selected.

For the ease of notation, we use A to represent $A(t)$. Consider the selection rule “if $\{A_1B, A_2B\}$ is selected, then $\{A_1, A_2, B\}$ must be selected”. Suppose for now all candidate variables are $\mathbb{V} = \{A_1, A_2, B, A_1B, A_2B\}$, which are the variables that are involved in this rule. According to Table 2 in²⁰, the selection dictionary (all permissible subsets of covariates that respect the selection dependency) is

$$\mathbb{D} = \{\emptyset, \{A_1, A_2\}, \{B\}, \{A_1, A_2, B\}, \{A_1, A_2, B, A_1B, A_2B\}\}.$$

Based on Theorem 5 in²⁰, we need to create groups whose complements (and their combinations) are equal to $\mathbb{D} \setminus \mathbb{V}$. We thus postulate three groups: $\{A_1, A_2, A_1B, A_2B\}$, $\{B, A_1B, A_2B\}$ and $\{A_1B, A_2B\}$, which satisfy the requirement. Similarly, to respect the selection dependency “if $\{C_1B, C_2B\}$ is selected, then $\{C_1, C_2, B\}$ must be selected”, we postulate another three groups $\{C_1, C_2, C_1B, C_2B\}$, $\{B, C_1B, C_2B\}$ and $\{C_1B, C_2B\}$.

However, the two rules share a same variable B : if either $\{A_1B, A_2B\}$ or $\{C_1B, C_2B\}$ is selected, then B must be selected. To satisfy this requirement, we need to merge the two groups $\{B, A_1B, A_2B\}$ and $\{B, C_1B, C_2B\}$ into one group $\{A_1B, A_2B, B, C_1B, C_2B\}$ to prevent the occurrence of rule-breaking combinations for example, $\{C_1B, C_2B\}$ being selected without B .

We also need to respect another selection rule: the dummy variables for a categorical variable need to be selected collectively. The categorical interaction variables AB and BC are already being selected collectively because of the above selection dependencies. However, additional groups for $\{A_1, A_2\}$ are unnecessary as this would make it possible to select $\{A_1B, A_2B\}$ without A . In addition, with the above groups, A_1 and A_2 would never be selected individually because they are always in a same group. Therefore, we have 5 defined groups listed below

$$\begin{aligned} \mathbb{G}_1 &= \{A_1, A_2, A_1B, A_2B\}, \mathbb{G}_2 = \{B, A_1B, A_2B, C_1B, C_2B\}, \\ \mathbb{G}_3 &= \{A_1B, A_2B\}, \mathbb{G}_4 = \{C_1, C_2, C_1B, C_2B\}, \mathbb{G}_5 = \{C_1B, C_2B\}. \end{aligned}$$

Our resulting selection dictionary is: $\{\emptyset, \{B\}, \{C_1, C_2\}, \{B, C_1, C_2\}, \{B, C_1, C_2, C_1B, C_2B\}, \{A_1, A_2\}, \{A_1B, A_2B, B\}, \{A_1, A_2, C_1, C_2\}, \{A_1, A_2, A_1B, A_2B, B\}, \{A_1, A_2, B, C_1, C_2\}, \{A_1, A_2, B, C_1, C_2, A_1B, A_2B\}, \{A_1, A_2, B, C_1, C_2, C_1B, C_2B\}, \{A_1, A_2, B, A_1B, A_2B, C_1, C_2, C_1B, C_2B\}\}$. The code to derived the selection dictionary using R is available at https://github.com/Guanbo-W/sox_sim. One can verify the correctness of the derived selection dictionary using Theorem 5 in²⁰.

D Additional simulation results for Section 5.2

See the results in Table D2

E Sample solution path

See Figure E1 for the sample solution path.

F Additional simulation: Comparison with existing sparse group lasso methods (additional simulations)

In this simulation, we compare our method, the sparse group LASSO, and the LASSO, implemented by `sox`, `SGL`, and `glmnet` respectively. We aim to show that `sox` can respect certain selection rules that `SGL` or `glmnet` cannot. We follow a similar setting as the one in Section 5.2 within the cases of $(n = 400/800, p = 210)$. Since `SGL` cannot handle time-dependent Cox models, we generate time-fixed covariates.

The sparse group LASSO, due to its inability to accommodate overlapping groups, does not adhere to the principle of strong heredity. To define its group structure, we have organized the groups in a specific manner: each of the 10 groups contains two consecutive main terms along with their interaction (we have 20 main terms, so 10 such groups are specified, each containing

Method	sox	sox.db	CoxL	CoxL.db	sox	sox.db	CoxL	CoxL.db	
$p = 210$		$n = 400$				$n = 800$			
JDR	0.15	0.05	0.00	0.00	0.45	0.00	0.40	0.05	
MR	0.17	0.28	0.30	0.37	0.05	0.15	0.05	0.13	
FAR	0.04	0.00	0.02	0.01	0.02	0.00	0.03	0.01	
R1S	1.00	1.00	0.98	0.99	1.00	1.00	0.98	0.99	
RCI	0.83	0.81	0.82	0.81	0.83	0.82	0.83	0.82	
MSE*	7.01	6.39	9.17	6.93	5.79	5.76	6.48	5.70	
CV-E	1.82	1.78	1.87	1.77	1.73	1.73	1.75	1.71	
$p = 465$		$n = 400$				$n = 800$			
MR	0.18	0.33	0.36	0.40	0.04	0.13	0.07	0.13	
FAR	0.02	0.00	0.01	0.01	0.01	0.00	0.01	0.00	
R1S	1.00	1.00	0.99	0.99	1.00	1.00	0.99	0.99	
RCI	0.84	0.81	0.83	0.81	0.83	0.82	0.83	0.82	
MSE*	3.22	2.85	3.71	3.00	2.63	2.55	3.14	2.58	
CV-E	1.83	1.78	1.87	1.74	1.71	1.71	1.76	1.70	
$p = 820$		$n = 400$				$n = 800$			
MR	0.20	0.31	0.40	0.45	0.04	0.18	0.10	0.16	
FAR	0.02	0.00	0.01	0.01	0.01	0.00	0.01	0.00	
R1S	1.00	1.00	0.99	0.99	1.00	1.00	0.99	0.99	
RCI	0.84	0.80	0.82	0.81	0.83	0.82	0.84	0.83	
MSE*	1.89	1.69	2.27	1.87	1.49	1.46	1.78	1.40	
CV-E	1.82	1.78	1.90	1.74	1.73	1.73	1.78	1.69	

Table D2 Simulation results of the high-dimensional case. In the tuning process, “lambda.1se” is used. Results are averaged over 20 independent replications. CoxL: unstructured ℓ_1 penalty (glmnet with "cox" family); sox: our method; .db: with additional debiasing procedure. JDR: joint detection rate, MR: missing rate, FAR: false alarm rate, R1S: rule 1 satisfaction, RCI: the C index of the model with the selected variables, MSE: mean-squared error (*values are multiplied by 10^{-3}), CV-E: cross-validated error.

three variables). Additionally, the 180 remaining interactions are each treated as individual groups. This configuration results in a total of 190 distinct groups.

The results, presented in Table F3, show that sox outperforms glmnet, consistent with the findings in Section 5.2. The inferior performance of glmnet is attributed to its inability to incorporate selection rules. In this simulation, a flawed grouping structure was applied to the sparse group LASSO, leading it to adhere to selection rules not aligned with the actual data generation mechanism. This situation parallels Bayesian analysis, where an incorrect prior leads to suboptimal outcomes, which explains why SGL demonstrates the least effective performance in this context.

G Additional simulation: Timing results.

Additionally, we also tested the computational speed of sox. We adopted the simulation setting from Section 5.2. For all (n, p) pairs, we reported the computation time (in seconds) for solving 10-fold cross-validation on the same λ sequence of length 30 in Table G4. The computation time of sox.db does not include the necessary procedures to acquire the initial estimates (sox in our case) used to calculate the regularization weights. Our findings indicate that for a complex case where the sample size is $n = 800$ and the number of variables is $p = 820$, a comprehensive analysis can be completed in approximately 10 minutes. In contrast, for a simpler scenario with a sample size of $n = 400$ and $p = 210$ variables, the analysis requires less than 30 seconds to finish.

Method	sox	sox.db	CoxL	CoxL.db	SGL	sox	sox.db	CoxL	CoxL.db	SGL
$p = 210$			$n = 400$			$n = 800$				
MR	0.04	0.05	0.06	0.08	0.02	0.00	0.01	0.00	0.00	0.18
FAR	0.32	0.22	0.17	0.14	0.76	0.34	0.24	0.22	0.18	0.40
R1S	1.00	1.00	0.89	0.91	0.81	1.00	1.00	0.87	0.90	0.87
RCI	0.84	0.84	0.84	0.84	0.88	0.82	0.82	0.82	0.82	0.72
MSE*	3.41	2.37	3.77	3.18	3727	2.21	1.50	2.37	1.80	3242
CV-E	5.51	5.34	5.52	5.30	48.02	5.48	5.38	5.48	5.36	53.14

Table F3 Simulation results of interaction selection under the time-fixed, high-dimensional setting. In the tuning process, “lambda.1se” is used. Results are averaged over 20 independent replications. CoxL: unstructured ℓ_1 penalty (glmnet with “cox” family); sox: our method; SGL: the sparse group LASSO; .db: with additional debiasing procedure. JDR: joint detection rate, MR: missing rate, FAR: false alarm rate, R1S: rule 1 satisfaction, RCI: the C index of the model with the selected variables, MSE: mean-squared error (*values are multiplied by 10^{-3}), CV-E: cross-validated error.

	$n = 400$		$n = 800$	
	sox	sox.db	sox	sox.db
$p = 210$	26.80	26.47	54.13	53.93
$p = 465$	121.39	114.12	217.95	217.11
$p = 820$	391.26	359.85	704.67	698.86

Table G4 Timing results of the high-dimensional case. Results are averaged over 20 independent replications.

H Additional simulation: Comparison of different group sizes, the amount of overlap, and the sparsity levels

In this section, we delved into how group size, the amount of overlap between groups, and sparsity level influence the performance of our method. We adopt a low-dimensional setting ($n = 400, p = 25$) time-dependent (with four time-points, and each variable held constant for two or three times-points). Each variable is independently generated by the standard Gaussian distribution. We investigate seven grouping structures with different group sizes and amount of overlap, the details of which are summarized in Table H5.

The results of the simulation are detailed in Table H6. A closer look at settings 1, 3, and 2, which feature groups of 10 variables each with similar sparsity but different overlap sizes (8, 5, and 2, respectively), reveals a decrease in false alarm rates. This trend is attributed to the fact that smaller overlaps reduce the probability of mistakenly selecting variables from both groups, thereby lowering the chances of misidentifying noise as a significant signal. Although setting 1 shows a slightly higher sparsity level, it does not substantially affect the outcome.

In contrast, settings 4, 3, and 5, which have identical overlap and sparsity levels but varying group sizes (13, 10, and 7, respectively), also show a declining trend in false alarm rates. This is because the selection of variables 14 and 15 may result in the selection of the variables in group 2. When group 2 has more variables, there is an increased risk of erroneously selecting them.

Regarding settings 5 to 7, where each group consists of 7 variables with an overlap size of 5 and varying sparsity levels for group 2 (0.7, 0.9, and complete sparsity or 1), settings 5 and 6 display similar false alarm rates. This is due to the possibility of a single signal in a group triggering the erroneous selection of all variables in that group. However, with complete sparsity, the false alarm rate tends to zero. Notably, setting 6 exhibits a significantly higher missing rate, possibly because a lone signal in group 2 (variable 14) is sometimes not strong enough for selection, leading to its omission.

These findings demonstrate that group size, overlap, and sparsity levels significantly influence the performance of sox. Nonetheless, caution should be exercised in generalizing these results, as variations in the data-generating mechanism can alter these conclusions.

	Variable index	1	2	3	4	5	6	7	8	9	10	11	12	13	14	15	16	17	18	19	20	21	22	23	24	25
Setting	True Coefficient	0	0	0	0	0	0	0	0	0	0	0	0	0	0.4	0.4	0.4	0	0	0.4	0	0	0.4	0	0	0
1	Group size 10 Overlap size 8	1	2	3	4	5	6	7	8	9	10	11	12	13	14	15	16	17	18	19	20	21	22	23	24	25
2	Group size 10 Overlap size 2	1	2	3	4	5	6	7	8	9	10	11	12	13	14	15	16	17	18	19	20	21	22	23	24	25
3	Group size 10 Overlap size 5	1	2	3	4	5	6	7	8	9	10	11	12	13	14	15	16	17	18	19	20	21	22	23	24	25
4	Group size 13 Overlap size 5	1	2	3	4	5	6	7	8	9	10	11	12	13	14	15	16	17	18	19	20	21	22	23	24	25
5	Group size 7* Overlap size 5	1	2	3	4	5	6	7	8	9	10	11	12	13	14	15	16	17	18	19	20	21	22	23	24	25
6	Group size 7** Overlap size 5	1	2	3	4	5	6	7	8	9	10	11	12	13	14	15	16	17	18	19	20	21	22	23	24	25
7	Group size 7*** Overlap size 5	1	2	3	4	5	6	7	8	9	10	11	12	13	14	15	16	17	18	19	20	21	22	23	24	25

Table H5 True coefficients and grouping structures for the simulation to evaluate the effects of group sizes and the amount of overlaps. In all seven settings, there is a group 1 in red and a group 2 in blue with their overlaps in purple. For the variables that are in neither groups 1 or 2, each belongs to a group of size one.

Setting	1	2	3	4	5	6	7
Overlap size	8	2	5	5	5	5	5
Group size	10	10	10	13	7	7	7
SL* of group 2	0.8	0.7	0.7	0.7	0.7	0.9	1
SL* of group 1	1	1	1	1	1	1	1
MR	0.01	0.00	0.01	0.01	0.00	0.11	0.00
FAR	0.36	0.30	0.31	0.46	0.17	0.17	0.01
RCI	0.76	0.76	0.76	0.76	0.76	0.75	0.76
MSE**	1.64	1.57	1.61	1.66	1.51	1.76	1.55
CV-E	1.90	1.89	1.89	1.89	1.88	1.91	1.88

Table H6 Simulation results for different group sizes and amount of overlap. * Sparsity Level; ** MSEs are multiplied by 10^{-2} .

I Inclusion and exclusion criteria

Figure I2 shows the inclusion and exclusion criteria for the patients of the study cohort.

J Covariate definitions

The 7 baseline covariates are 1) Age ($\geq 75/ < 75$), 2) Sex(female/male), 3) CHA2DS2VASc ($\geq 3/ < 3$), 4) Diabetes, 5) COPD/asthma, 6) Hypertension and 7) Malignant cancer. All other covariates are time-dependent covariates.

Heart disease: including 1) valvular heart disease, 2) peripheral vascular disease, 3) cardiovascular disease, 4) chronic heart failure, and 5) myocardial infarction.

DOAC: it is 1 if the patient uses DOAC, 0 if the patient is taking warfarin or not taking any OAC at the time t .

OAC: it is 1 if the patient uses OAC, 0 if the patient is not taking any OAC at the time t .

High-dose-DOAC: it is 1 if the patient uses high-dose-DOAC, 0 if the patient is taking low-dose-DOAC, or warfarin or not taking any OAC at the time t .

Antiplatelets: ASA low dose (≥ 80 mg and ≤ 260 mg), dipyridamole or clopidogrel or ticlopidine or prasugrel or ticagrelor.

Statin: Statin or other lipid lowering drugs.

NASIDs: Nonsteroidal anti-inflammatory drugs.

K Summary statistics of all the covariates

Table K7 gives the summary statistics of all the covariates stratified by if the subject experienced the event (death) during the follow-up. All the covariates in this analysis are binary variables. The first two columns (% at cohort entry) show the summary statistics of the covariates at the time of cohort entry. The second two columns (% of value changed) show, for each covariate, the percentage of patients who experienced situation change during the follow-up. The third two columns (% mean over population and time) show, for each covariate, the average value of the covariates across all patients during the follow-up (the mean, over the population, of the values of the covariates during the follow-up).

Covariate	% at cohort entry		% of value changed		% mean	
Age (≥ 75)	67	82	0	0	66	82
Sex(female/male)	54	52	0	0	54	52
Comorbidities/Medical score						
$CHA_2DS_2VAS_c$ (≥ 3)	80	89	0	0	79	88
Diabetes	34	39	0	0	34	39
COPD/asthma	35	51	0	0	35	49
Hypertension	81	84	0	0	81	84
Malignant cancer	23	36	0	0	23	36
Stroke	19	16	3	5	21	18
Chronic kidney disease	33	53	6	14	36	58
Heart disease	66	80	7	9	70	83
Major bleeding	28	38	9	18	33	45
OAC use						
DOAC	61	51	58	47	54	38
Apixaban	31	29	26	25	27	22
Dabigatran	11	7	13	8	10	5
OAC	100	100	91	94	83	70
High-dose-DOAC	39	23	41	23	34	17
Concomitant medication use						
Antiplatelets	52	59	43	34	24	37
NSAIDs	7	5	11	6	3	3
Statin	54	52	11	11	53	49
Beta-Blockers	65	63	18	12	62	62
Potential drug-drug interaction						
DOAC: Antiplatelets	27	25	30	27	10	11
DOAC: NSAIDs	4	3	7	4	2	1
DOAC: Statin	30	23	33	24	29	18
DOAC: Beta-Blockers	38	30	40	32	34	22

Table K7 Summary statistics of the baseline and time-dependent covariates

L Analysis using the time-dependent Cox model

Table L8 provides the crude (univariate) and adjusted hazard ratios from simple and multivariate time-dependent Cox models for death, respectively, and 95% confidence intervals using the covariates in the analysis.

Covariate	Crude HR		Adjusted HR	
	Estimate	CI	Estimate	CI
Age (≥ 75)	2.25	(2.09, 2.44)	1.89	(1.73, 2.06)
Sex(female/male)	0.92	(0.86, 0.97)	0.98	(0.92, 1.04)
Comorbidities/Medical score				
CHA2DS2VASc (≥ 3)	2.00	(1.82, 2.20)	1.01	(0.90, 1.14)
Diabetes	1.23	(1.16, 1.31)	1.08	(1.02, 1.15)
COPD/asthma	1.84	(1.74, 1.96)	1.49	(1.40, 1.58)
Hypertension	1.20	(1.10, 1.30)	0.91	(0.83, 0.99)
Malignant cancer	1.79	(1.68, 1.90)	1.45	(1.36, 1.54)
Stroke	1.07	(1.00, 1.15)	1.00	(0.92, 1.07)
Chronic kidney disease	3.50	(3.29, 3.73)	2.10	(1.96, 2.25)
Heart disease	3.42	(3.11, 3.76)	2.41	(2.18, 2.67)
Major bleeding	2.55	(2.40, 2.70)	1.38	(1.29, 1.47)
OAC use				
DOAC	0.06	(0.06, 0.07)	1.60	(1.16, 2.21)
Apixaban	0.11	(0.09, 0.13)	0.88	(0.68, 1.14)
Dabigatran	0.09	(0.07, 0.12)	0.77	(0.53, 1.13)
OAC	0.03	(0.02, 0.03)	0.84	(0.66, 1.06)
High-dose-DOAC	0.07	(0.06, 0.08)	0.80	(0.63, 1.01)
Concomitant medication use				
Antiplatelets	1.37	(1.28, 1.47)	0.80	(0.74, 0.86)
NSAIDs	1.14	(0.97, 1.33)	1.50	(1.27, 1.76)
Statin	0.70	(0.66, 0.75)	0.82	(0.76, 0.87)
Beta-Blockers	0.92	(0.87, 0.98)	1.37	(1.28, 1.47)
Potential drug-drug interaction				
DOAC: Antiplatelets	0.11	(0.09, 0.15)	1.09	(0.81, 1.47)
DOAC: NSAIDs	0.15	(0.09, 0.26)	0.99	(0.56, 1.78)
DOAC: Statin	0.08	(0.07, 0.09)	0.90	(0.70, 1.15)
DOAC: Beta-Blockers	0.08	(0.09, 0.10)	0.60	(0.47, 0.77)

Table L8 Crude (univariate) and adjusted hazard ratios from simple and multivariate time-dependent Cox models for death, respectively, and 95% confidence intervals using the covariates in the analysis.

M Rational of the selection rules

Selection rules 1 and 2: rule 1 is needed since when DOAC is in the model, and if Apixaban is selected, then the interpretation of the coefficient of Apixaban is the contrast of Apixaban and Rivaroxaban. If High-dose-DOAC is also in the model, the interpretation would be the contrast (e.g. log hazard ratio) of low-dose-Apixaban versus low-dose Rivaroxaban. However, without DOAC, the coefficient of Apixaban would represent a contrast against warfarin and Rivaroxaban combined, which is less interpretable. The same rationale applies to Dabigatran in rule 2.

Selection rule 3: it is needed because when OAC is in the model, and if DOAC is selected, then the interpretation of the coefficient of DOAC is the contrast of DOAC and warfarin. However, without OAC, the coefficient of DOAC would represent a contrast against DOAC and warfarin or taking none of OAC combined, which is less interpretable.

Selection rule 4: it is needed since when DOAC is in the model, and if High-dose-DOAC is selected, then the interpretation of the coefficient of High-dose-DOAC is the contrast of high-dose-DOAC versus low-dose-DOAC, which is of interest. If Apixaban and Dabigatran are also in the model, the coefficient of High-dose-DOAC represents the contrast between high-dose-Rivaroxaban versus low-dose-Rivaroxaban. However, without DOAC in the model, these relevant interpretations would be lost.

N Grouping structure of the data analysis

In our method, we need to specify the grouping structure to respect the selection rules. Thirteen variables are included in the 8 selection rules. For the convenience of grouping structure specification, we denote the 13 variables as such:

A: Apixaban, B: Dabigatran, C: High-dose-DOAC, D: DOAC: Antiplatelets, E: DOAC: NSAIDs, F: DOAC: Statin, G: DOAC: Beta-Blockers, H: DOAC, I: Antiplatelets, J: NSAIDs, K: Statin, L: Beta-Blockers, M: OAC.

According to^{20,58}. The grouping structure that relevant to these 13 variables should be

$$\begin{aligned} \mathfrak{G}_1 &= \{A\}, \mathfrak{G}_2 = \{B\}, \mathfrak{G}_3 = \{C\}, \mathfrak{G}_4 = \{D\}, \mathfrak{G}_5 = \{E\}, \mathfrak{G}_6 = \{F\}, \mathfrak{G}_7 = \{G\}, \mathfrak{G}_8 = \{D, I\}, \\ \mathfrak{G}_9 &= \{E, J\}, \mathfrak{G}_{10} = \{F, K\}, \mathfrak{G}_{11} = \{G, L\}, \mathfrak{G}_{12} = \{A - H\}, \mathfrak{G}_{13} = \{A, B, C, H, M\}, \end{aligned}$$

13 groups in total. For the remaining 11 variables, each of them has one individual group. Therefore, we have 24 groups in total. For the 13 groups, we plot the grouping structure in Figure N3. We can see that it presents a graph structure. Multiple groups are overlapped with and nested in other groups.

To encode the grouping structure into our developed software, we need to specify two matrices, both of which are 24 by 24 matrices. The first matrix has 1 in the positions (4, 8), (5, 9), (6, 10), (7, 11), (1, 12), (2, 12), (3, 12), (4, 12), (5, 12), (6, 12), (7, 12), (1, 13), (2, 13), (3, 13), the rest are 0. The second matrix has 1 in the positions $(i, i), i = 1, \dots, 7, 13, \dots, 24, (9, 8), (10, 9), (11, 10), (12, 11), (8, 12), (8, 13)$, the rest are 0. For details, please see the help file in the R package.

O Visualization of the analysis

We artificially create three hypothetical patients' disease progression. Suppose person 1, age ≥ 75 , who only used the drug warfarin, had only malign cancer among all the disease variables included in the data. Person 2 has the same profile as person 1 except they ceased warfarin at time 100 during the follow-up, while other statuses stayed the same. Person 3 developed major bleeding at time 200, and all other statuses were the same as person 2. Figure O4 shows the survival curves of the three people, estimated by the time-dependent Cox model using the covariates that were selected by our method. As we can see, person 1 (in red) has the highest estimated survival probability. The survival probability of person 2 drops immediately after the cease of warfarin. Similarly, the survival probability drops significantly at time 200 due to the major bleeding. Note that Figure O4 only intends to show, as an example, how the survival probability can vary according to time-dependent covariates, rather than predicting the survival probability of the hypothetical cases. All the covariates involved in the study are internal covariates that relate to the outcome in the sense that the covariates can be measured only among the patients who are still at risk of the event (alive).

References

1. Reid N, Cox D. *Analysis of survival data*. Chapman and Hall/CRC . 2018.
2. Holcomb JB, others . The prospective, observational, multicenter, major trauma transfusion (PROMMTT) study: comparative effectiveness of a time-varying treatment with competing risks. *JAMA surgery* 2013; 148(2): 127–136.
3. Weisz G, others . Ranolazine in patients with incomplete revascularisation after percutaneous coronary intervention (RIVER-PCI): a multicentre, randomised, double-blind, placebo-controlled trial. *The Lancet* 2016; 387(10014): 136–145.

4. Huang J, Sun T, Ying Z, Yu Y, Zhang CH. Oracle inequalities for the lasso in the Cox model. *Annals of statistics* 2013; 41(3): 1142.
5. Fan J, Li R. Variable selection for Cox's proportional hazards model and frailty model. *Annals of Statistics* 2002: 74–99.
6. Beretta A, Heuchenne C. Variable selection in proportional hazards cure model with time-varying covariates, application to US bank failures. *Journal of Applied Statistics* 2019; 46(9): 1529–1549.
7. Yan J, Huang J. Model selection for Cox models with time-varying coefficients. *Biometrics* 2012; 68(2): 419–428.
8. Lim M, Hastie T. Learning interactions via hierarchical group-lasso regularization. *Journal of Computational and Graphical Statistics* 2015; 24(3): 627–654.
9. Wang L, Shen J, Thall PF. A modified adaptive Lasso for identifying interactions in the Cox model with the heredity constraint. *Statistics & probability letters* 2014; 93: 126–133.
10. Simon N, Friedman J, Hastie T, Tibshirani R. A sparse-group lasso. *Journal of computational and graphical statistics* 2013; 22(2): 231–245.
11. Wang S, Nan B, Zhu N, Zhu J. Hierarchically penalized Cox regression with grouped variables. *Biometrika* 2009; 96(2): 307–322.
12. Dang X, Huang S, Qian X. Penalized cox's proportional hazards model for high-dimensional survival data with grouped predictors. *Statistics and Computing* 2021; 31: 1–27.
13. Obozinski G, Jacob L, Vert JP. Group lasso with overlaps: the latent group lasso approach. *arXiv preprint arXiv:1110.0413* 2011.
14. Villa S, Rosasco L, Mosci S, Verri A. Proximal methods for the latent group lasso penalty. *Computational Optimization and Applications* 2014; 58: 381–407.
15. Jenatton R, Audibert JY, Bach F. Structured variable selection with sparsity-inducing norms. *The Journal of Machine Learning Research* 2011; 12: 2777–2824.
16. Lian Y, Wang G, Yang AY, et al. *sox: Structured Learning in Time-Dependent Cox Models*. 2023. R package version 1.0.
17. Breslow N. Covariance analysis of censored survival data. *Biometrics* 1974: 89–99.
18. Kim J, Sohn I, Jung SH, Kim S, Park C. Analysis of survival data with group lasso. *Communications in Statistics-Simulation and Computation* 2012; 41(9): 1593–1605.
19. Yan X, Bien J, others . Hierarchical sparse modeling: A choice of two group lasso formulations. *Statistical Science* 2017; 32(4): 531–560.
20. Wang G, Schnitzer ME, Chen T, Wang R, Platt RW. A general framework for formulating structured variable selection. *arXiv* 2023.
21. Mairal J, Jenatton R, Obozinski G, Bach F. Convex and Network Flow Optimization for Structured Sparsity.. *Journal of Machine Learning Research* 2011; 12(9).
22. Boyd S, Vandenberghe L. *Convex optimization*. Cambridge university press . 2004.
23. Moreau JJ. Fonctions convexes duales et points proximaux dans un espace hilbertien. *Comptes rendus hebdomadaires des séances de l'Académie des sciences* 1962; 255: 2897–2899.
24. Combettes PL, Pesquet JC. Proximal splitting methods in signal processing. In: Springer. 2011 (pp. 185–212).
25. Bach F. Structured sparsity-inducing norms through submodular functions. *Advances in Neural Information Processing Systems* 2010; 23.
26. Beck A, Teboulle M. A fast iterative shrinkage-thresholding algorithm for linear inverse problems. *SIAM journal on imaging sciences* 2009; 2(1): 183–202.
27. Nesterov Y. Gradient methods for minimizing composite objective function. CORE Discussion Papers 2007076, Université catholique de Louvain, Center for Operations Research and Econometrics (CORE); 2007.
28. Beck A. *First-order methods in optimization*. 25. SIAM . 2017.
29. Jenatton R, Mairal J, Obozinski G, Bach F. Proximal methods for hierarchical sparse coding. *Journal of Machine Learning Research* 2011; 12(Jul): 2297–2334.
30. Bertsekas D. *Network optimization: continuous and discrete models*. 8. Athena Scientific . 1998.
31. Ford LR, Fulkerson DR. Maximal flow through a network. *Canadian journal of Mathematics* 1956; 8: 399–404.
32. Babenko M, Goldberg AV. Experimental evaluation of a parametric flow algorithm. *Technical Report MSR-TR-2006-77* 2006.
33. Mairal J, Bach F, Ponce J. Sparse modeling for image and vision processing. *arXiv preprint arXiv:1411.3230* 2014.
34. Therneau TM. *A Package for Survival Analysis in R*. 2021. R package version 3.2-10.

35. Friedman J, Hastie T, Tibshirani R. Regularization paths for generalized linear models via coordinate descent. *Journal of statistical software* 2010; 33(1): 1.
36. Simon N, Friedman J, Hastie T, Tibshirani R. Regularization paths for Cox's proportional hazards model via coordinate descent. *Journal of statistical software* 2011; 39(5): 1.
37. Goldberg AV, Tarjan RE. A new approach to the maximum-flow problem. *Journal of the ACM (JACM)* 1988; 35(4): 921–940.
38. Cherkassky BV, Goldberg AV. On implementing the push—relabel method for the maximum flow problem. *Algorithmica* 1997; 19(4): 390–410.
39. Bertsekas DP. Nonlinear programming. *Journal of the Operational Research Society* 1997; 48(3): 334–334.
40. Chen Y, Yang Y. The One Standard Error Rule for Model Selection: Does It Work?. *Stats* 2021; 4(4): 868–892.
41. Zhang Z, others . Time-varying covariates and coefficients in Cox regression models. *Annals of translational medicine* 2018; 6(7).
42. R Core Team . *R: A Language and Environment for Statistical Computing*. R Foundation for Statistical Computing; Vienna, Austria: 2021.
43. Sylvestre MP, Evans T, MacKenzie T, Abrahamowicz M. *PermAlgo: Permutational algorithm to generate event times conditional on a covariate matrix including time-dependent covariates*. 2010. R package version 1.1.
44. She Y, Wang Z, Jiang H. Group regularized estimation under structural hierarchy. *Journal of the American Statistical Association* 2018; 113(521): 445–454.
45. Simon N, Friedman J, Hastie T, Tibshirani R. *SGL: Fit a GLM (or Cox Model) with a Combination of Lasso and Group Lasso Regularization*. 2019. R package version 1.3.
46. Dang X. *grpCox: Penalized Cox Model for High-Dimensional Data with Grouped Predictors*. 2020. R package version 1.0.1.
47. Jacob L, Obozinski G, Vert JP. Group lasso with overlap and graph lasso. In: ; 2009: 433–440.
48. Obozinski G, Jacob L, Vert JP. Group lasso with overlaps: the latent group lasso approach. *arXiv preprint arXiv:1110.0413* 2011.
49. Kropko J, Harden J. *coxed: Duration-Based Quantities of Interest for the Cox Proportional Hazards Model*. 2020. R package version 0.3.3.
50. Lip GY, Tse HF. Management of atrial fibrillation. *The Lancet* 2007; 370(9587): 604–618.
51. Angiolillo DJ, others . Antithrombotic therapy in patients with atrial fibrillation treated with oral anticoagulation undergoing percutaneous coronary intervention: a North American perspective: 2021 update. *Circulation* 2021; 143(6): 583–596.
52. Claxton JS, others . A new model to predict major bleeding in patients with atrial fibrillation using warfarin or direct oral anticoagulants. *PLoS one* 2018; 13(9): e0203599.
53. Perreault S, others . Oral anticoagulant prescription trends, profile use, and determinants of adherence in patients with atrial fibrillation. *Pharmacotherapy: The Journal of Human Pharmacology and Drug Therapy* 2020; 40(1): 40–54.
54. Fauchier L, others . Cause of death in patients with atrial fibrillation admitted to French hospitals in 2012: a nationwide database study. *Open Heart* 2015; 2(1): e000290.
55. Fauchier L, others . Causes of death and influencing factors in patients with atrial fibrillation. *The American journal of medicine* 2016; 129(12): 1278–1287.
56. Lee E, others . Mortality and causes of death in patients with atrial fibrillation: a nationwide population-based study. *PLoS One* 2018; 13(12): e0209687.
57. Harb SC, others . CHA2DS2-VASc score stratifies mortality risk in patients with and without atrial fibrillation. *Open Heart* 2021; 8(2): e001794.
58. Wang G, Perreault S, Platt RW, Wang R, Dorais M, Schnitzer ME. Integrating complex selection rules into the latent overlapping group Lasso for constructing coherent prediction models. *arXiv preprint arXiv:2206.05337* 2023.
59. Kalbfleisch JD, Prentice RL. *The statistical analysis of failure time data*. 360. John Wiley & Sons . 2011.
60. Zhang CH. Nearly unbiased variable selection under minimax concave penalty. *The Annals of statistics* 2010; 38(2): 894–942.
61. Fan J, Li R. Variable selection via nonconcave penalized likelihood and its oracle properties. *Journal of the American statistical Association* 2001; 96(456): 1348–1360.

62. Siddique AA, Schnitzer ME, Bahamyirou A, et al. Causal inference with multiple concurrent medications: A comparison of methods and an application in multidrug-resistant tuberculosis. *Statistical methods in medical research* 2019; 28(12): 3534–3549.
63. Wang G, Schnitzer ME, Menzies D, Viiklepp P, Holtz TH, Benedetti A. Estimating treatment importance in multidrug-resistant tuberculosis using Targeted Learning: An observational individual patient data network meta-analysis. *Biometrics* 2020; 76(3): 1007–1016.
64. Liu Y, Schnitzer ME, Wang G, et al. Modeling treatment effect modification in multidrug-resistant tuberculosis in an individual patient data meta-analysis. *Statistical methods in medical research* 2022; 31(4): 689–705.
65. Wang G, Poulin-Costello M, Pang H, et al. Evaluating hybrid controls methodology in early-phase oncology trials: A simulation study based on the MORPHEUS-UC trial. *Pharmaceutical Statistics* 2023; n/a(n/a). doi: <https://doi.org/10.1002/pst.2336>
66. Wang G. Review 1: "Antibiotic Prescribing in Remote Versus Face-to-Face Consultations for Acute Respiratory Infections in English Primary Care: An Observational Study Using TMLE". *Rapid Reviews Infectious Diseases* 2023.
67. Bouchard A, Bourdeau F, Roger J, et al. Predictive Factors of Detectable Viral Load in HIV-Infected Patients. *AIDS Research and Human Retroviruses* 2022; 38(7): 552–560.
68. Haris A, Witten D, Simon N. Convex Modeling of Interactions With Strong Heredity. *Journal of Computational and Graphical Statistics* 2016; 25(4): 981–1004. doi: 10.1080/10618600.2015.1067217
69. Reisberg B, others . The Global Deterioration Scale for assessment of primary degenerative dementia.. *The American journal of psychiatry* 1982.
70. Zhai T, Gu H, Yang Y. Cox regression based modeling of functional connectivity and treatment outcome for relapse prediction and disease subtyping in substance use disorder. *Frontiers in Neuroscience* 2021; 15: 768602.
71. Lee YB, others . Sparse SPM: Group Sparse-dictionary learning in SPM framework for resting-state functional connectivity MRI analysis. *NeuroImage* 2016; 125: 1032–1045.
72. Chklovskii DB, Koulakov AA. Maps in the brain: what can we learn from them?. *Annu. Rev. Neurosci.* 2004; 27: 369–392.
73. Ward Jr JH. Hierarchical grouping to optimize an objective function. *Journal of the American statistical association* 1963; 58(301): 236–244.
74. Jenatton R, Gramfort A, Michel V, et al. Multiscale mining of fMRI data with hierarchical structured sparsity. *SIAM Journal on Imaging Sciences* 2012; 5(3): 835–856.

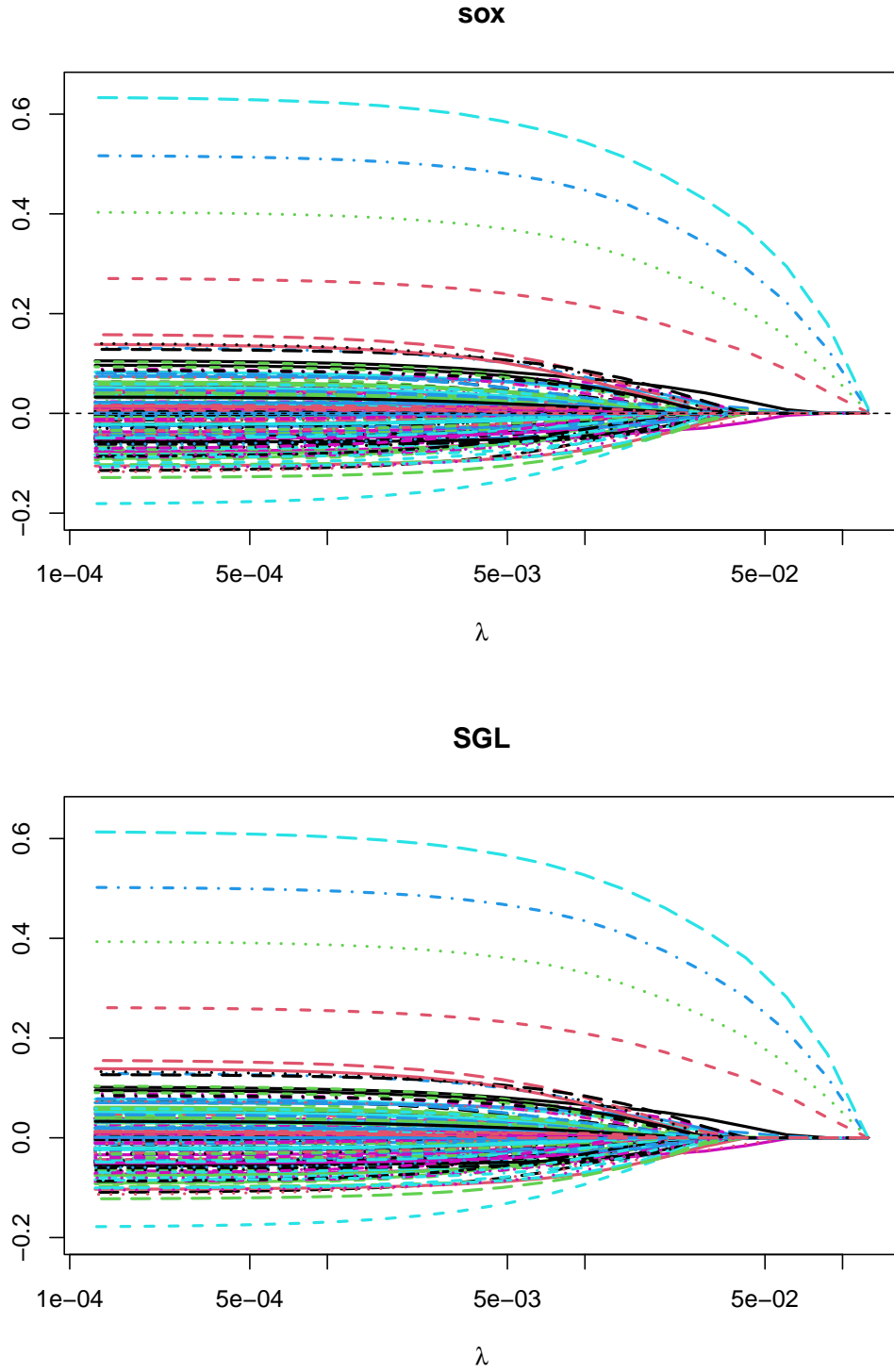


Figure E1 Sample solution paths from sox and SGL using the same data and the same λ sequence.

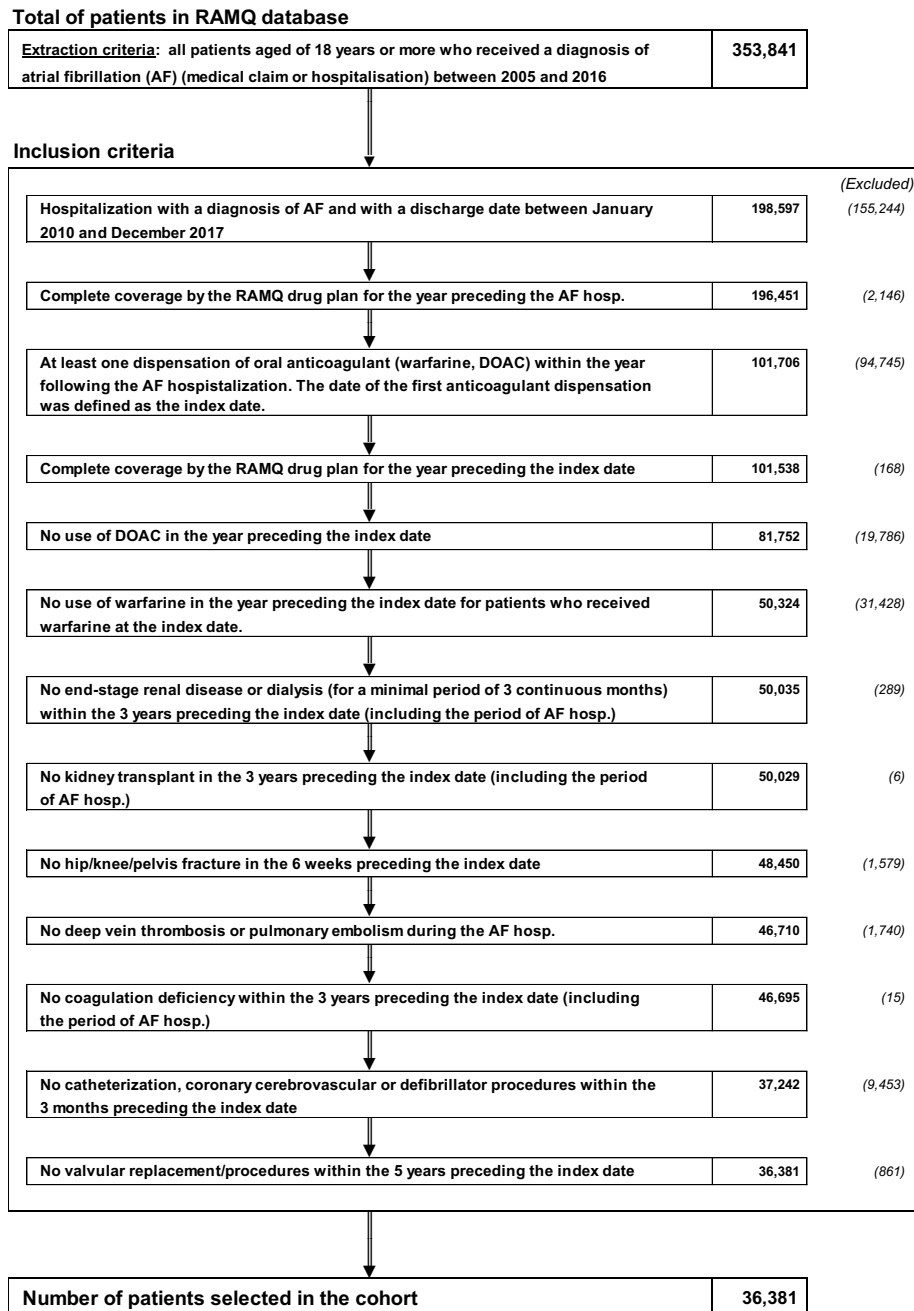


Figure 12 The inclusion and exclusion criteria for the patients of the study cohort. (AF: atrial fibrillation; OAC: oral anticoagulants).

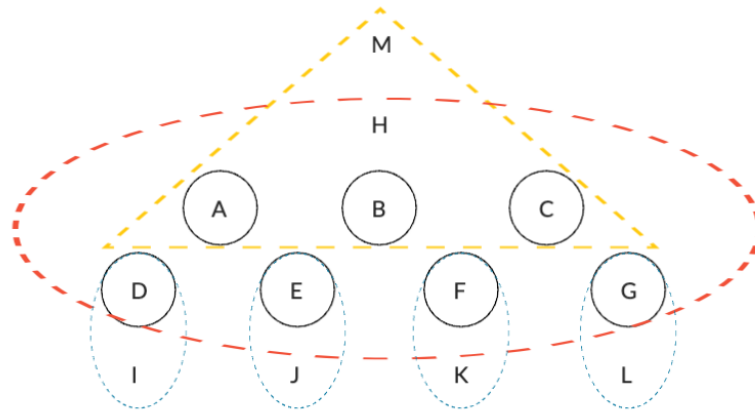


Figure N3 Grouping structure plot for the 13 groups

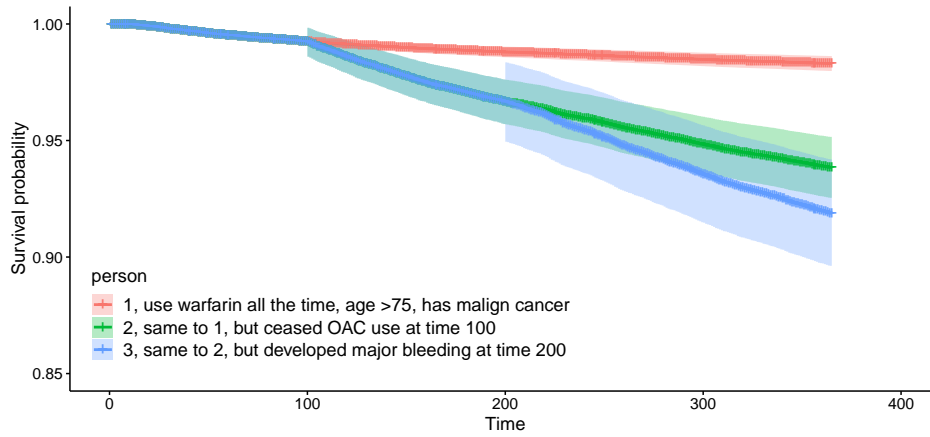


Figure O4 Estimated survival curves of three typical persons.